

國立交通大學

機械工程學系  
碩士論文

高解析度距離都普勒雷達成像流程研究

Research of High Resolution Range-Doppler Radar Imaging



研究生：侯俊仰

指導教授：成維華 教授

中華民國九十六年七月

# 高解析度距離都普勒雷達成像流程研究

Research of High Resolution Range-Doppler Radar Imaging Procedure

研究生：侯俊仰

Student : Ching-Yang Hou

指導教授：成維華

Advisor : Dr. Wei-Hua Chieng

國立交通大學

機械工程學系



Submitted to Institute of Mechanical Engineering  
College of Engineering  
National Chiao Tung University  
in partial Fulfillment of the Requirements  
for the Degree of  
Master  
in

Mechanical Engineering

July 2007

Hsinchu, Taiwan, Republic of China

中華民國九十六年七月

# 高解析度距離都普勒雷達成像流程研究

研究生：侯俊仰

指導教授：成維華 教授

國立交通大學機械工程學系

## 摘 要

距離都普勒雷達可以對距離軸與方位軸產生地面的二維影像，距離都普勒雷達所產生地面影像的品質決定於解析度的尺寸，而解析度尺寸可由距離與方位解析度來明確說明。好的距離解析度可以由脈波壓縮技術來獲得，而方位解析度則跟天線尺寸與工作波段的波長有關。在雷達的距離處理程序中常用匹配濾波器來得到最大的訊雜比訊號輸出並利用線性頻率調變來達到脈波壓縮的效果。在方位處理程序中即是利用天線本體的運動對待測物體的都普效應來產生線性調變的效果。故距離成像及方位成像處理程序有相同的數學模型，卻有截然不同的物理特徵及意義。基於距離壓縮與方位壓縮的原理，本篇論文主要是研究點目標模擬來建構出條帶式微波成像流程。

# Research of High Resolution Range-Doppler Radar Imaging Procedure

Student : Ching-Yang Hou

Advisor : Dr. Wei-Hua Chieng

Institute of Mechanical Engineering  
National Chiao Tung University

## Abstract

Range-Doppler radar can produce two-dimension imagery of the ground surface versus range and azimuth axis. The quality of ground maps generated by Range-Doppler radar is determined by the size of the resolution cell. A resolution cell is specified by both range and azimuth resolution of the system. Fine range resolution can be accomplished by using pulse compression techniques. The azimuth resolution depends on antenna size and radar wavelength of operation band. In radar range processing, it usually emphasizes the signal to noise ratio to be maximum and utilizes the linear frequency modulation to accomplish the pulse compression. However, it is utilizing the motion of antenna versus the Doppler effect of targets to produce the purpose of linear frequency modulation in azimuth processing.

The range and azimuth processing have the same mathematical modal, but have the different physical characteristics and meaning. Basing on the principle of range compression and azimuth compression, the main purpose is to construct a procedure of Strip-map microwave radar by using simulation of point target in this paper.

## 誌謝

首先要感謝我的指導老師 成維華 教授，讓我加入了實驗室，在這兩年的碩士生涯中，無論是在學業、生活、或是待人處事等方面，都不厭其煩的給予我指導與教誨，也從中獲得了啟發與智慧，在我踏入社會之前，給了我嚴格的磨練，我相信在近入職場後，有自信去面對各種問題，且都能找出解決的方法。

這個研究的完成，特別要感謝楊嘉豐學長對我的指導，對於反應不快的我，依然是很有耐心地把我從無教到有，在這兩年裡，也因學長亦師亦友的指導，我才能順利的畢業。

實驗室的氣氛一直都是很愉快地，很高興能認識童永成學長、張仰宏學長、以及吳秉霖學長，因為學長們的熱情，讓我感到實驗室的溫馨，偉鈞、明亮、明欣、建成，跟你們一起渡過了兩年吃喝拉撒吃喝拉睡都在一起的生活，這段同甘共苦的日子，我相信一定很難忘懷，情和義，值千金。

謝謝我的父母能夠支持我選擇的路，在這段日子裡，無論是生活或是心理方面，都能完完全全的支持我，而我也沒有讓你們失望，得到了碩士學位，謝謝你們，我只想跟你們說：「爸、媽，我在這裡，我畢業了」。也謝謝我的女朋友，我最艱困的日子裡，依然無怨無悔的陪在我身邊。

最後感謝所有曾經幫助過我的人以及我在交大認識的朋友，謝謝你們。

# Contents

摘要.....	i
<b>Abstract</b> .....	ii
誌謝.....	iii
<b>Contents</b> .....	iv
<b>List of Figures</b> .....	v
<b>List of Tables</b> .....	vii
<b>Chapter 1 Introduction</b> .....	1
1.1 History.....	1
1.2 Motive and Object.....	2
1.3 Research Orientation.....	3
<b>Chapter 2 Range processing</b> .....	4
2.1 Basic of Range Processing.....	4
2.1.1 Range Resolution.....	4
2.1.2 Linear Frequency Modulation Waveforms.....	5
2.1.3 Correlation and Convolution.....	6
2.2 The Matched Filter.....	8
2.3 LFM Pulse Compression.....	9
2.3.1 Correlation Processor.....	12
2.3.2 Time Interval of Sampling.....	15
2.3.3 Range Sampling Criteria.....	18
2.4 Simulation for Range Processing.....	19
<b>Chapter 3 Azimuth processing</b> .....	20
3.1 Azimuth Resolution.....	20
3.2 Properties of Echo Signal.....	22
3.3 Azimuth Compression.....	28
3.4 Azimuth Sampling Criteria.....	30
3.5 Simulation for Azimuth Processing.....	31
<b>Chapter 4 Stripmap Range-Doppler Radar Imaging Procedure</b> .....	32
4.1 Raw Data.....	32
4.2 Imaging Procedure.....	33
4.3 Simulation for Point Target.....	34
4.4 Compensation with Variable PRF.....	34
<b>Chapter 5 Conclusion</b> .....	36
<b>References</b> .....	37

## List of Figures

Figure 2-1	(a) Two unresolved targets. (b) Two resolved targets.....	38
Figure 2-2	Typical LFM waveforms. (a) Up-chirp; (b) Down-chirp.....	38
Figure 2-3	Correlation.....	39
Figure 2-4	Relationship between Multiplication and Convolution.....	39
Figure 2-5	Convolution.....	40
Figure 2-6	Matched filter definitions.....	40
Figure 2-7	Ideal LFM pulse compression.....	41
Figure 2-8	LFM pulse after matched filter.....	41
Figure 2-9	Computing the matched filter output using an FFT.....	42
Figure 2-10	System geometry for range imaging.....	42
Figure 2-11	Scenery of example in range processing.....	43
Figure 2-12	First method of range processing.....	43
Figure 2-13	Second method of range processing.....	43
Figure 2-14	Real part and spectrum of transmit signal.....	44
Figure 2-15	Real part and spectrum of reference signal.....	44
Figure 2-16	Receive signal and Compressed echo signal.....	45
Figure 3-1	Application of airborne Range-Doppler radar.....	45
Figure 3-2	Airborne Range-Doppler radar Geometry.....	46
Figure 3-3	Properties of frequency and phase between transmit signal and echo signal.....	46
Figure 3-4	Relationship between target location and Doppler frequency	47
Figure 3-5	Scenery of example in azimuth processing.....	47
Figure 3-6	Real part and spectrum of reference signal in azimuth direction.	48
Figure 3-7	Receive signal and compressed signal in azimuth direction.....	48
Figure 4-1	Transmitted and received signal in Range-Doppler radar.....	49
Figure 4-2	The diagram of raw data.....	49
Figure 4-3	Fast correlation with one-dimensional reference signal.....	50
Figure 4-4	Range-Doppler radar imaging procedure.....	50
Figure 4-5	Raw data with one point target.....	51
Figure 4-6	Image after range compression and correction.....	51
Figure 4-7	Range-Doppler radar image with one target.....	52
Figure 4-8	-4dB Contour for one point target.....	52
Figure 4-9	Range-Doppler radar image in azimuth with one target.....	53
Figure 4-10	Range-Doppler radar image in ground range direction.....	53
Figure 4-11	Raw data with multiple target.....	54
Figure 4-12	Range-Doppler radar image with multiple targets.....	54

Figure 4-13	-4dB Contour with multiple targets with multiple targets.....	55
Figure 4-14	The motion error between actual and nominal trajectory.....	55
Figure 4-15	The diagram of fixed PRF and variable PRF.....	56
Figure 4-16	The Scenery illuminated by Range-Doppler radar.....	56
Figure 4-17	Actual and nominal flight path.....	57
Figure 4-18	The image after range compression with nominal path.....	58
Figure 4-19	Range-Doppler radar image with nominal path.....	58
Figure 4-20	Range-Doppler radar image with actual path.....	59
Figure 4-21	Range-Doppler radar image after LOS compensation.....	59





## List of Tables

Table 2-1	Parameters for range processing.....	60
Table 3-1	Parameters for azimuth processing.....	60
Table 4-1	Parameters for one point target simulation.....	61
Table 4-2	Parameters for multiple point target simulation.....	61
Table 4-3	Parameters for scenery simulation.....	62



# Chapter 1 Introduction

The word radar is an abbreviation for RAdio Detection And Ranging. In general, radar system use modulated waveforms and directive antennas to transmit electromagnetic energy into a specific volume in space to search for targets. Objects within a search volume will reflect portions of this energy back to the radar. These echoes are then processed by the radar receiver to extract target information such as range, velocity, angular position, and target identifying characteristics.

## 1.1 Historical Reviews



The Synthetic Aperture Radar (SAR) concept is usually attributed to Carl Wiley of Goodyear Aircraft Corporation in 1951 (and subsequently patented in 1965 [Wiley, 1965]). However its first experimental validation was carried out in 1953 by a group of scientists at the University of Illinois (Sherwin et al., 1962); later on, the U.S. Army commissioned Project Wolverine on this subject to the University of Michigan. The University of Illinois, General Electric Company, Philco, Varian, and Goodyear Aircraft Corporation joined the project. This was the beginning of a series of activities that contributed to the development of SAR techniques.

The first operational SAR system is believed to be built in 1957 by Willow Run Laboratories of the University of Michigan (currently

Environmental Research Institute of Michigan [ERIM]) for the U.S. Department of Defense [DoD]. A large part of early activities in this field is still classified, and related information is not available. However, starting from the end of the 1960s, NASA began to sponsor the development of SAR systems for civilian applications. One of the first consisted of the modification of a system originally developed by ERIM and was declassified at the end of the 1960s. This system was later upgraded by NASA in 1973 by the addition of an L-band.

## **1.2 Motive and Object**

SAR imaging technique is related with electronic engineering, computer science and digital signal processing. The appearing and development of SAR enlarge the traditional radars' application. With the development of SAR imaging technique and the improvement of SAR imaging quality, high range and azimuth resolution has come true. As a result, SAR has been an important tool for scientific research and remote sensing. It will take on a supreme future in both military and economy.

Radar users and designers alike seek to accomplish high resolution by minimizing range resolution and azimuth resolution. In order to achieve high range resolution one must use very short pulses and consequently reduce the average transmitted power and impose severe operating bandwidth requirements. High resolution SAR requires more complex hardware implementation and costs very much. Before constructing the hardware of SAR, simulation is useful and

helpful to make the system more complete. For this reason, it is necessary to analyze and test through the simulation of airborne Strip-map SAR system.

### **1.3 Research Orientation**

This paper introduces firstly the basic principle behind one-dimensional range imaging via utilization of a radar bandwidth in chapter 2. Result shows that the algorithm to matched filtering imaging is very good by analyzed, because the signal matched to the echo of targets includes not only phase but amplitude information. Basing on this, the algorithm about azimuth imaging via utilization of a synthetic aperture is analogized in chapter 3. These basic principles, and their associated data acquisition and digital signal processing issues, will assist us in developing more concrete high resolution SAR.

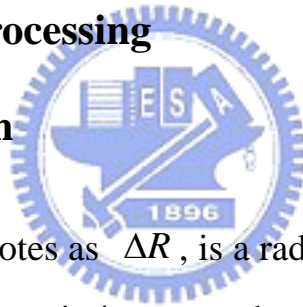
Chapter 4 discusses system modeling and imaging for broadside strip-map SAR within the framework of the spectral properties of the SAR radiation pattern that is developed in chapter 3. At the same time, the conclusion is validated by use of computer simulation. Then, the relationship between the trajectory and resolution can be analyzed as a result of the strip-map SAR modeling.

## Chapter 2 Procedure of Range Processing

For older radar systems where no pulse compression was possible, the range resolution was improved by reducing the pulse length. The disadvantage is that the transmitted power is also decreased which is directly linked to the signal to noise ratio (SNR). By instead transmitting frequency modulated pulses and using pulse compression techniques, the pulse length can be increased and still achieve fine range resolution.

### 2.1 Basics of Range Processing

#### 2.1.1 Range Resolution



Range resolution, denoted as  $\Delta R$ , is a radar metric that describes its ability to detect targets in close proximity to each other as distinct objects. Targets separated by at least  $\Delta R$  will be completely resolved in range.

Assume that the two targets are separated by  $cT_p/4$ , where  $T_p$  is the pulsewidth. In this case, when the pulse trailing edge strikes target 2 the leading edge would have traveled backwards a distance  $cT_p$ , and the returned pulse would be composed of returns from both targets, as shown in Fig. 2-1a. However if the two targets are at least  $cT_p/2$  apart, then as the pulse trailing edge strikes the first target the leading edge will start to return from target 2, and two distinct returned pulses will be produced, as illustrated by Fig. 2-1b. Thus,

$\Delta R$  should be greater or equal to  $cT_p/2$ . And since the radar bandwidth  $B$  is equal to  $1/T_p$ , then

$$\Delta R = \frac{cT_p}{2} = \frac{c}{2B} \quad (2-1)$$

## 2.1.2 Linear Frequency Modulation Waveforms

Frequency or phase modulated waveforms can be used to achieve much wider operating bandwidths. Linear Frequency Modulation (LFM) <sup>[1]</sup> is commonly used. In this case, the frequency is swept linearly across the pulsewidth, either upward (up-chirp) or downward (down-chirp). The matched filter bandwidth is proportional to the sweep bandwidth, and is independent of the pulsewidth. Fig. 2-2 shows a typical example of an LFM waveform. The pulsewidth is  $T_p$ , and the bandwidth is  $B$ .

The LFM up-chirp instantaneous phase can be expressed by

$$\psi(t) = 2\pi\left(f_c t + \frac{k}{2}t^2\right) \quad -\frac{T_p}{2} \leq t \leq \frac{T_p}{2} \quad (2-2)$$

where  $f_c$  is the radar center frequency, and  $K = (2\pi B)/\tau$  is the LFM coefficient. Thus, the instantaneous frequency is

$$f(t) = \frac{1}{2\pi} \frac{d}{dt} \psi(t) = f_0 + kt \quad -\frac{T_p}{2} \leq t \leq \frac{T_p}{2} \quad (2-3)$$

Atypical LFM waveform can be expressed by

$$s_1(t) = \text{Rect}\left(\frac{t}{T_p}\right) e^{j2\pi\left(f_c + \frac{k}{2}t^2\right)} \quad (2-4)$$

where  $\text{Rect}\left(\frac{t}{T_p}\right)$  denotes a rectangular pulse of width  $T_p$ .

### 2.1.3 Correlation and Convolution

Correlation<sup>[2]</sup> is the process of matching two waveforms, usually in the time domain, to determine their degree of fit and to determine the time at which the maximum correlation coefficient, or best fit, occurs. Correlation can occur in either the continuous or discrete realms.

This correlation from involves signals which are continuous and periodic. A mathematical description of continuous correlation is

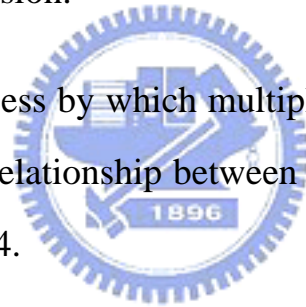
$$z(t) = x(t) \otimes h(t) = \int_{-\infty}^{\infty} x(\tau)h(t + \tau)d\tau \quad (2-5)$$

In the process, one signal  $[x(\tau)]$  is hold stationary in time and the other  $[h(t + \tau)]$  is displaced in time and slides across it. At each point in the displacement, or sliding, process, the product of  $x$  and  $h$  is taken and the area under the product found. This area is the correlation of  $x$  and  $h$  at time. The variable tau ( $\tau$ ) is time for purposes of finding the area under the product.

The parameter  $t$  represents the amount of displacement of  $h$  from its normal time position where  $t=0$ . Note that on the right of the equation,  $t$  is a parameter; on the left, it is a variable. Thus the process is truly a transform in that it changes the independent variable. The correlation process is shown in Fig. 2-3.

Two types of correlation exist. If the two waves being matched are different,  $x(t) \neq h(t)$ , a cross-correlation is performed. If they are the same,  $x(t) = h(t)$ , it is an autocorrelation. Autocorrelation are used to evaluation the suitability of waveforms to certain radar tasks and cross-correlation are used primarily in pulse compression.

Convolution is a process by which multiplications are transferred from one domain to the other. The relationship between multiplication and convolution is given below and in Fig. 2-4.



$$FT[f(t) \cdot w(t)] = FT[f(t)] * FT[w(t)] = F(f) * W(f) \quad (2-6)$$

The process of convolution is almost identical to that of correlation. The only difference is that one of the signals (it makes no difference which one) is reversed, or folded, in time before the displace-multiply-integrate operations. Convolution of continuous functions is given below

$$z(t) = x(t) * h(t) = \int_{-\infty}^{\infty} x(\tau)h(t - \tau)d\tau \quad (2-7)$$

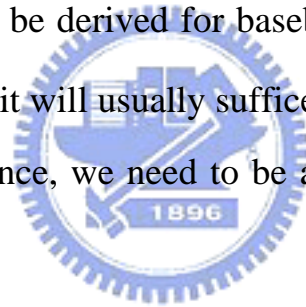
Graphically, convolution is shown in Fig. 2-5. Note its similarity to correlation as in Fig. 2-3; the only difference is time-reversal of  $h$ .



## 2.2 The Matched Filter

In radar applications we generally utilize the reflected known signal to detect the existence of a reflecting target. The probability of detection is related to the signal to noise ratio (SNR) rather than to the exact waveform of the signal received. Hence we are more interested in maximizing the SNR than in preserving the shape of the signal. A specific matched filter is a linear filter whose impulse response is determined by a specific signal in a way that will result in the maximum attainable SNR at the output of the filter when that particular signal and white noise are passed through the filter.

Matched filter<sup>[3]</sup> can be derived for baseband as well as for bandpass real signals. For the latter case it will usually suffice to implement a filter matched to the complex of signal. Hence, we need to be able to design matched filters for complex signals as well.



The impulse response of the matched filter is

$$h(t) = Ks^*(t_0 - t) \quad (2-8)$$

This says that the impulse response is a delayed mirror image of the conjugate of the signal.

It can easily be derived using convolution between the signal and the matched filter impulse response,

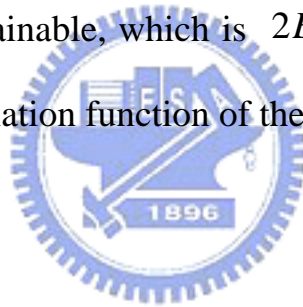
$$s_o(t) = s(t) * h(t) = \int_{-\infty}^{\infty} s(\tau)h(t - \tau)d\tau = \int_{-\infty}^{\infty} s(\tau)Ks^*[t_0 - (t - \tau)]d\tau \quad (2-9)$$

If we assume that  $t_0 = 0$  and  $K = 1$ , then

$$s_o(t) = \int_{-\infty}^{\infty} s(\tau)s^*(\tau - t)d\tau \quad (2-10)$$

the right-hand side of Eq. (2-10) is recognized as the autocorrelation function of  $s(t)$ .

We can now summarize the main results concerning the matched filter: The impulse response is linearly related to the time-inverted complex-conjugate signal; when the input to the matched filter is the correct signal plus white noise, the peak output response is linearly related to the signal's energy. At that instance, the SNR is the highest attainable, which is  $2E/N_0$ ; elsewhere, the response is described by the autocorrelation function of the signal.



### 2.3 LFM Pulse Compression

Linear frequency modulation pulse compression is accomplished by adding frequency modulation to a long pulse at transmission, and by using a matched filter receiver in order to compress the received signal.

The matched filter impulse response of  $s(t)$  is

$$h(t) = s^*(-t) \quad (2-11)$$


Substituting Eq. (2-4) into Eq. (2-11) yields

$$h(t) = \text{Rect}\left(\frac{t}{T_p}\right) e^{j2\pi f_c t} e^{-j\pi k t^2} \quad (2-12)$$

Then, the output signal  $s_o(t)$  of  $s(t)$  passing through the system  $h(t)$  is

$$\begin{aligned} s_o(t) &= s(t) * h(t) \\ &= \int_{-\infty}^{\infty} s(u) h(t-u) du \\ &= \int_{-\infty}^{\infty} h(u) s(t-u) du \\ &= \int_{-\infty}^{\infty} \text{Rect}\left(\frac{t}{T_p}\right) e^{j2\pi f_c u} e^{-j\pi k u^2} x \text{Rect}\left(\frac{t}{T_p}\right) e^{j2\pi f_c (t-u)} e^{j\pi k (t-u)^2} du \end{aligned}$$

When  $-T_p \leq t \leq 0$ ,



$$\begin{aligned} s_o(t) &= \int_{-T}^{t+T} e^{j\pi k t^2} e^{-j2\pi k t u} du \\ &= e^{j\pi k t^2} \frac{e^{-j2\pi k t u}}{-j2\pi k t} \Big|_{-T}^{t+T} e^{j2\pi f_c t} \\ &= \frac{\sin \pi k (2T + t)t}{\pi k t} \end{aligned} \quad (2-13)$$

When  $0 \leq t \leq T_p$ ,

$$s_o(t) = \int_{t-T}^T e^{j\pi k t^2} e^{-j2\pi k t u} du$$

$$\begin{aligned}
&= e^{j\pi kt^2} \frac{e^{-j2\pi ktu}}{-j2\pi kt} \Big|_{t-T}^T e^{j2\pi f_c t} \\
&= \frac{\sin \pi k(2T-t)t}{\pi kt}
\end{aligned} \tag{2-14}$$

Combining Eq. (2-13) with Eq. (2-14) yields

$$s_o(t) = T \frac{\sin \pi kT(1-\frac{|t|}{T})t}{\pi kTt} \text{Rect}(\frac{t}{2T}) e^{j2\pi f_c t} \tag{2-15}$$

Eq. (2-15) is the output of LFM signal passing through the matched filter. It is a signal of fixed carrier frequency  $f_c$ .

When  $t \leq T_p$ , the envelope is similar to a sinc function

$$s_o(t) = TSa(\pi kTt) \text{Rect}(\frac{t}{2T}) = TSa(\pi Bt) \text{Rect}(\frac{t}{2T}) \tag{2-16}$$

As illustrated in Fig. 2-7,  $t = \pm \frac{1}{B}$  is the first zero point when  $\pi Bt = \pm \pi$ ;

When  $\pi Bt = \pm \frac{\pi}{2}$ ,  $t = \pm \frac{1}{2B}$ . It is usually to define the presently pulsewidth as

the compressed pulsewidth

$$\tau = \frac{1}{2B} \times 2 = \frac{1}{B} \tag{2-17}$$

As a result, the matched filter output is compressed by a factor  $\xi = BT_p$ , where  $\tau'$  is the pulsewidth and  $B$  is the bandwidth. Thus, by using long pulses and wideband LFM modulation large compression ratio can be achieved.

The time axis is normalized in Fig. 2-8,  $(t/(1/B) = t \times B)$ . The result simulated in Fig. 2-8 is as good as the theory. The relative amplitude is -13.4 dB when the first zero point appears at  $\pm 1 (\pm \frac{1}{B})$ . As illustrated in Fig. 2-9, it is equal to the analysis in theory and the relative amplitude is -4dB when the compressed pulsewidth is similar to  $\frac{1}{B} (\pm \frac{1}{2B})$ .



### 2.3.1 Correlation Processor

Radar operations are usually carried out over a specified range window, referred to as the receive window and defined by the difference between the radar maximum and minimum range. Returns from all targets within the receive window are collected and passed through matched filter circuitry to perform pulse compression. One implementation of such analog processors is the Surface Acoustic Wave (SAW) devices. Because of the recent advances in digital computer development, the correlation processor<sup>[4]</sup> is often performed digitally using FFT. This digital implementation is called Fast Convolution Processing (FCP) and can be implemented at base-band. The fast convolution process is illustrated in Fig. 2-9.

Since the matched filter is a linear time invariant system, its output can be described mathematically by the convolution between its input and its impulse response,

$$y(t) = s(t) * h(t) \quad (2-18)$$

where  $s(t)$  is the input signal,  $h(t)$  is the matched filter impulse response(reference signal), and the  $*$  operator symbolically represents convolution. From the Fourier transform properties,

$$FFT\{s(t) * h(t)\} = S(f) \cdot H(f) \quad (2-19)$$

and when both signals are sampled properly, the compressed signal  $y(t)$  can be computed from

$$y(t) = FFT^{-1}\{S(f) \cdot H(f)\} \quad (2-20)$$

where  $FFT^{-1}$  is the inverse FFT. When using pulse compression, it is desirable to use modulation schemes that can accomplish a maximum pulse compression ratio, and can significantly reduce the sidelobe levels of the compressed waveform. For the LFM case the first sidelobe is approximately 13.4dB below the main peak, and for most radar applications this may not be sufficient. In practice, high sidelobe levels are not preferable because noise and/or jammers located at the sidelobes may interfere with target returns in the main lobe.

Weighting function (windows) can be used on the compressed pulse spectrum in order to reduce the sidelobe levels. The cost associated with such an approach is a loss on the main lobe resolution, and a reduction in the peak value. Weighting the time domain transmitted or received signal instead of the compressed pulse spectrum will theoretically achieve the same goal. However, this approach is rarely used, since amplitude modulating the transmitted waveform introduces extra burdens on the transmitter.

Consider a radar system that utilizes a correlation processor receiver. The receive window in meters is defined by

$$R_{\text{rec}} = R_{\text{max}} - R_{\text{min}} \quad (2-21)$$

where  $R_{\text{max}}$  and  $R_{\text{min}}$ , respectively, define the maximum and minimum range over which the radar performs detection. Typically  $R_{\text{rec}}$  is limited to extent of the target complex. The normalized complex transmitted signal has the form

$$s(t) = \exp \left[ j2\pi \left( f_c t + \frac{k}{2} t^2 \right) \right] \quad 0 \leq t \leq T_p \quad (2-22)$$

$T_p$  is the pulsewidth,  $k = B/T_p$ , and B is the bandwidth.

The radar echo signal is similar to the transmitted one with the exception of a time delay and an amplitude change that correspond to the target RCS. Consider a target at range  $R_1$ . The echo received by the radar from this target is

$$s_r(t) = a_1 \exp \left[ j2\pi \left( f_c(t - \tau_1) + \frac{k}{2}(t - \tau_1)^2 \right) \right] \quad \tau_1 \leq t \leq \tau_1 + T_p \quad (2-23)$$

where  $a_1$  is proportional to target RCS, antenna gain, and range attenuation.

The time delay  $\tau_1$  is given by

$$\tau_1 = 2R_1 / c \quad (2-24)$$

The first step of the processing consists of removing the frequency  $f_c$ .

This is accomplished by missing  $s_r(t)$  with a reference signal whose phase is  $2\pi f_c t$ . The phase of the resultant signal, after low pass filtering, is then given

by

$$\psi(t) = 2\pi \left[ -f_c \tau_1 + \frac{k}{2}(t - \tau_1)^2 \right] \quad (2-25)$$

and the instantaneous frequency is

$$f_i(t) = \frac{1}{2\pi} \frac{d}{dt} \psi(t) = k(t - \tau_1) = \frac{B}{T_p} \left( t - \frac{2R_1}{c} \right) \quad (2-26)$$

### 2.3.2 Time Interval of Sampling

The spatial domain shown as Fig. 2-10 support band of the target is



$$x \in [x_c - x_0, x_c + x_0]$$

where  $x_c$  is the target area mean range and  $2x_0$  is the size of the target area.

The echoed signal from the closest reflector at  $x = x_c - x_0$  arrives at the time

$$t_{start} = \frac{2(x_c - x_0)}{c} \quad (2-27)$$

While the echoed signal from the farthest reflector at  $x = x_c + x_0$  arrives at the receiver at the time  $2(x_c + x_0)/c$ , it lasts until the time

$$t_{end} = \frac{2(x_c + x_0)}{c} + T_p \quad (2-28)$$

where  $T_p$  is the duration of the pulsed radar signal. The echoed signals that are due to the reflectors that reside between the closest and farthest reflectors fall between the time points  $T_{start}$  and  $T_{end}$ .

Thus, to capture the echoed signals from all of the reflectors in the target region  $x \in [x_c - x_0, x_c + x_0]$ , we have to acquire the time samples of the echoed signal in the following time interval<sup>[5]</sup>:

$$t \in [t_{start}, t_{end}]$$

Note that the length of this time interval is

$$t_{end} - t_{start} = \frac{4x_0}{c} + T_p \quad (2-29)$$

### 2.3.3 Range Sampling Criteria

The number of samples,  $N$ , must be chosen so that foldover in the spectrum is avoided. For this purpose, the sampling frequency,  $f_s$  based on the Nyquist sampling rate, must be

$$f_s \geq 2B \quad (2-30)$$

and the sampling interval is



$$T_s \leq \frac{1}{2B} \quad (2-31)$$

Using Eq. (2-26) it can be show that the frequency resolution of the FFT is

$$\Delta f \leq \frac{1}{T_p} \quad (2-32)$$

The minimum required number of samples is


$$N = \frac{1}{\Delta f T_s} = \frac{T_p}{T_s} \quad (2-33)$$

Equating Eqs. (2-31) and (2-33) yields

$$N \geq 2BT_p \quad (2-34)$$

Consequently, a total of  $2BT_p$  real samples, or  $BT_p$  complex samples, is sufficient to completely describe an LFM waveform of duration  $T_p$  and bandwidth  $B$ . For example, an LFM signal of duration  $T_p = 2\mu s$  and bandwidth  $B = 10MHz$  requires 40 real samples to determine the input signal.

For better implementation of the FFT  $N$  is extended to the next power of two, by zero padding. Thus, the total number of samples, for some positive integer  $m$ , is

$$N_{FFT} = 2^m \geq N \quad (2-35)$$


## 2.4 Simulation for Range Processing

As an example shown as Fig. 2-11, consider the case where the parameters are list in table 2-1. The simulation of range processing can be achieved by using MATLAB as Fig. 2-12, and the reference signal is

$$s_{ref}(t) = \exp\left(j\pi k(t - \tau_r)^2\right) \quad \tau_r \leq t \leq \tau_r + T_p \quad (2-36)$$

The  $\tau_r$  is given by

$$\tau_r = \frac{2R_{mid}}{c} \quad (2-37)$$

where  $R_{mid}$  is the center distance of receive window.

Because of the properties of Fourier transform

$$F\{s(t)\} = S(w) \quad (2-38)$$

$$F\{s(-t)\} = -S(-w) \quad (2-39)$$

$$F\{s^*(t)\} = S^*(-w) \quad (2-40)$$

It can be known that

$$F\{s^*(-t)\} = -S^*(w) \quad (2-41)$$

The simulation can be achieved by another way illustrated in Fig. 2-13.

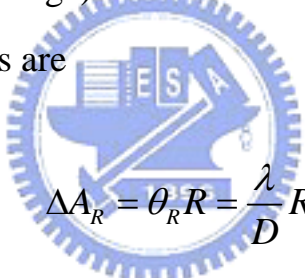
Note that the compressed pulse range resolution is ten meters. Figs. 2-14 and 2-15 show the transmit signal and reference signal respectively. Fig 2-16 shows the uncompressed echo and the compressed matched filter output.

## Chapter 3 Azimuth Processing

SAR synthesizes a long antenna by transmitting electromagnetic energy and coherently adding the successively reflected and received pulses to obtain high resolution in azimuth direction. To achieve a coherent integration is called azimuth compression.

### 3.1 Azimuth Resolution

Azimuth (cross-range) is resolved with antenna beamwidth. The azimuth resolution of radars are



$$\Delta A_R = \theta_R R = \frac{\lambda}{D} R \quad (3-1)$$

$$\Delta A_S = \theta_S R = \frac{\lambda}{2L_{syn}} R \quad (3-2)$$

where  $\Delta A_R$  is the azimuth resolution using the real antenna,  $\Delta A_S$  is the azimuth resolution using the synthetic antenna,  $\theta_R$  and  $\theta_S$  are the 3-dB beamwidth of the real antenna and synthetic antenna respectively,  $D$  is the width of the real antenna,  $L_{syn}$  is the effective length of the synthetic antenna,  $\lambda$  is the wavelength, and  $R$  is the range to the targets being resolved.

Azimuth resolution is enhanced by narrowing the antenna beamwidth. With real antennas, this requires enlarging the physical antenna size or decreasing wavelength, which are often not possible because of physical constraints. The same effect can be accomplished with a small real antenna moving to a number of locations to simulate a large antenna, called a synthetic, or synthetic aperture as illustrated in Fig. 3-1.

The azimuth resolution of a sidelooking SAR system is described in terms of the geometry of Fig. 3-2. The effective length of the synthetic antenna ( $L_{syn}$ ) is the distance the radar moves while a scatterer remains in the beam. It has the same value as the azimuth resolution of the real antenna. For small real beamwidths, this value is



$$\Delta A_R = L_{syn} = \theta_R R = \frac{\lambda}{D} R \quad (3-3)$$

The azimuth resolution of the synthetic antenna at range  $R$  is, by basic resolution relationships

$$\Delta A_S = \theta_S R \quad (3-4)$$

Substituting Eq. (3-2) into Eq. (3-4) yields

$$\Delta A_S = \frac{\lambda R}{2L_{syn}} \quad (3-5)$$

Substituting Eq. (3-3) into Eq. (3-5) yields

$$\Delta A_s = \frac{\lambda R}{2} \frac{D}{R\lambda} \quad (3-6)$$

Algebra reduces this equation to

$$\Delta A_s = \frac{D}{2} \quad (3-7)$$

### 3.2 Properties of Echo Signal

In order to make it convenient for the mathematic analysis, the geometry of airborne SAR<sup>[6]</sup> should be discussed firstly. As illustrated in Figs. 3-1 and 3-2, the aircraft flies along the straight line in  $x$  direction with uniform velocity  $v$  and altitude  $h$ . The antenna of airborne SAR transmits the radio waves broadside with regular slant angle  $\beta$ . Assume that the 3dB beamwidth is  $\theta$ , the measured swath is  $W$ , the maximum synthetic aperture length is  $L$ .

The detected target is assumed as a ideal point target  $p$  and the slant range between target  $p$  and flight path  $x$  is  $R_0$ . Therefore, the coordinate plane can be composed of flight path  $x$  and slant range  $R_0$ . The aircraft is in the origin of coordinate when  $t=0$  and the location of aircraft is  $x=vt$  in instantaneous time  $t$ . The location of point target  $p$  in this coordinate is fixed and its coordinate is  $(x_p, R_0)$ . In instantaneous time  $t$ , the distance  $R$  between antenna and target  $p$  is

$$R = \sqrt{R_0^2 + (x_a - x_p)^2} \quad (3-8)$$

In general,  $R_0 \gg (x_a - x_p)$ , the equation above is similar to

$$R = R_0 \sqrt{1 + \frac{(x_a - x_p)^2}{R_0^2}} \approx R_0 + \frac{(x_a - x_p)^2}{2R_0} \quad (3-9)$$

The high frequency pulse which is transmitted from the antenna is periodic and coherent equally amplitude. Suppose the frequency is  $f_c$ , the amplitude is  $A$ , the pulse repetition frequency (PRF) is  $f_r$ , the repetition period (PRT) is  $T_r = \frac{1}{f_r}$ , and the pulsewidth is  $\tau$ . The first step is assuming the signal transmitted from antenna is a continuous cosine wave for analysis. The actual transmitted periodic pulse is viewed as the samples of continuous wave and its sampling frequency is PRF  $f_r$ . The amplitude of cosine wave is normalized as 1 and the beginning phase is 0. As a result, It can be expressed by using exponential function with complex number

$$S_0(t) = e^{j2\pi f_c t} \quad (3-10)$$

The signal after transmitted from antenna is a type of electromagnetic wave. When arriving the target  $p$ , the electromagnetic wave is started to scatter, and a part of backscatter energy is received by antenna, thus, being called echo signal  $S_r(t)$ . Assume that the RCS of point target  $p$  is  $\sigma$ ,  $S_r(t)$  can be expressed by



$$S_r(t) = \sigma e^{j2\pi f_c(t-\tau_0)} \quad (3-11)$$


where  $\tau_0$  is the two-way time delay, that means

$$\tau_0 = \frac{2R}{c} \quad (3-12)$$

Substituting Eq. (3-9) into Eq. (3-12) yields

$$\tau_0 = \frac{2}{c} \left[ R_0 + \frac{(x_a - x_p)^2}{2R_0} \right] = \frac{2R_0}{c} + \frac{(x_a - x_p)^2}{cR_0} \quad (3-13)$$

Substituting Eq. (3-13) into Eq. (3-11), the echo signal can be expressed by



$$S_r(t) = \sigma e^{j2\pi f_c \left( t - \frac{2R_0}{c} + \frac{(x_a - x_p)^2}{cR_0} \right)} \quad (3-14)$$

After simplified and normalized, we get

$$S_r(t) = e^{j2\pi f_c t} e^{-j\frac{4\pi R_0}{\lambda}} e^{-j\frac{2\pi(x_a - x_p)^2}{\lambda R_0}} \quad (3-15)$$

where  $\lambda$  denotes transmitted wave length ( $\lambda = \frac{c}{f_c}$ ). Choosing the real part and

making it to become the form of cosine function

$$S_r(t) = \cos \left[ 2\pi f_c t - \frac{4\pi R_0}{\lambda} - \frac{2\pi(x_a - x_p)^2}{\lambda R_0} \right] \quad (3-16)$$

Observing the phase of this signal, it is composed of three terms and can be written as

$$\phi = \phi_1 + \phi_2 + \phi_3 \quad (3-17)$$

where  $\phi_1 = 2\pi f_c t$  is the linear phase term of the original signal,  $\phi_2 = -\frac{4\pi R_0}{\lambda}$

is the phase term changes with  $R_0$  and has nothing to do with time. For the targets with same slant range,  $R_0$  is constant and  $\phi_2$  is a constant phase that

can be neglected when observing variation of phase.  $\phi_3 = -\frac{2\pi(x_a - x_p)^2}{\lambda R_0}$  is the

most important phase term and is the key in technique of SAR signal processing.

And  $x = vt$ ,  $x_p = vt_p$ , where  $t_p$  denotes the among of time which the aircraft spend in arriving the location  $x_p$  that the target  $p$  exists. Thus  $\phi_3$  can also be expressed by

$$\phi_3 = -\frac{2\pi v^2 (t - t_p)^2}{\lambda R_0} \quad (3-18)$$

It is the quadratic phase term changing with time in the presence of square-law, where  $v$  is the velocity of aircraft. Differentiating the phase with respect to time time, then divided by  $2\pi$ , the instantaneous frequency can be obtained

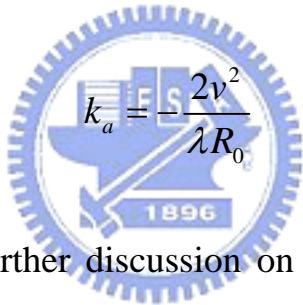
$$f_r = \frac{1}{2\pi} \frac{d}{dt} \left[ 2\pi f_c t - \frac{4\pi R_0}{\lambda} - \frac{2\pi(x_a - x_p)^2}{\lambda R_0} \right]$$

$$= f_c t - \frac{2v^2}{\lambda R_0} (t - t_p) \quad (3-19)$$

where  $f_c$  is the carrier frequency of transmitted signal. The second is the Doppler history caused from the relative motion between antenna and target and it is usually denoted as

$$f_d = -\frac{2v^2}{\lambda R_0} (t - t_p) \quad (3-20)$$

It changes with time linearly and it is perceived that the echo signal is a linear frequency modulation waveform where the chirp rate is

$$k_a = -\frac{2v^2}{\lambda R_0} \quad (3-21)$$


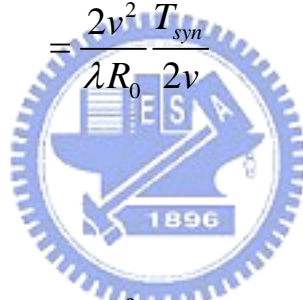
For the convenience of further discussion on the property of echo signal, the variation of phase and frequency of echo signal was compared with that of transmit signal as illustrated in Fig. 3-3.

As shown in Eq. (3-20) and Fig. 3-3, the Doppler shift caused from point target  $p$  ranges between negative and positive with a center at  $t = t_p$ . When  $t = t_p$ , the antenna will be located at the slant range between flying path and target  $p$ . The quantity of aircraft velocity  $v$  along the direction of target  $p$  is the radial velocity and is equal to zero. Before  $t = t_p$ ,  $f_d$  is positive and its maximum value occurs at

$$t = t_p - \frac{L_{syn} / 2}{v} = t_p - \frac{T_{syn}}{2} \quad (3-22)$$

where  $L_{syn}$  is the synthetic aperture length of target  $p$  and  $T_{syn}$  is the synthetic aperture interval. At this moment, the Doppler shift is

$$\begin{aligned} f_{d1} &= -\frac{2v^2}{\lambda R_0} \left( t_p - \frac{L_{syn}}{2v} - t_p \right) \\ &= \frac{2v^2}{\lambda R_0} \frac{L_{syn}}{2v} \\ &= \frac{2v^2}{\lambda R_0} \frac{T_{syn}}{2v} \end{aligned} \quad (3-23)$$



After  $t = t_p$ ,  $t - t_p$  is positive,  $f_d$  is negative and its most negative value occurs at

$$t = t_p + \frac{L_{syn} / 2}{v} = t_p + \frac{T_{syn}}{2} \quad (3-24)$$

At this moment, the Doppler shift is

$$\begin{aligned} f_{d1} &= -\frac{2v^2}{\lambda R_0} \left( t_p + \frac{L_{syn}}{2v} - t_p \right) \\ &= -\frac{2v^2}{\lambda R_0} \frac{L_{syn}}{2v} \end{aligned}$$

$$= -\frac{2v^2}{\lambda R_0} \frac{T_{syn}}{2v} \quad (3-25)$$

The bandwidth of Doppler history of target  $p$  can be obtained From either Eqs. (3-23) and (3-25) or Fig. 3-3, namely,

$$\Delta f_d = f_{d1} - f_{d2} = \frac{2v^2}{\lambda R_0} T_{syn} = \frac{2v}{\lambda R_0} L_{syn} \quad (3-26)$$

### 3.3 Azimuth Compression

Assume that there are two targets  $p_1$ 、 $p_2$  on the ground. They are identical to the vertical slant range of the flying path, both being  $R_0$ . However their azimuth is different. As illustrated in Fig. 3-4, their coordinate in x direction are  $x_1$  and  $x_2$  respectively. According to the previous discussion, the echo signal of two targets are both linear modulation signal and their bandwidth is equal to their Doppler shift that is

$$\Delta f_d = \frac{2v^2}{\lambda R_0} T_{syn} \quad (3-27)$$

But It is different to start and end of the Doppler frequency. In frequency domain, the instantaneous frequency of two echo signal is not the same time. When the location of aircraft is  $x = vt$ , the instantaneous frequency of first echo signal is

$$f_{d1} = -\frac{2v}{\lambda R_0}(x - x_1) \quad (3-28)$$

and the instantaneous frequency of first echo signal is

$$f_{d2} = -\frac{2v}{\lambda R_0}(x - x_2) \quad (3-29)$$

The difference of both Doppler frequency is

$$f_{d2} - f_{d1} = \frac{2v}{\lambda R_0}(x_1 - x_2) = \frac{2v}{\lambda R_0} \Delta x \quad (3-30)$$

If the difference can be recognized, the distance between two targets can be resolved either.

In the technique of radio, the method that can solve this problem is called correlation and the procedure of autocorrelation is equal to the matched filter. If the linear modulation of echo signal is used in matched filter, the output is presented as a sinc function and it is called azimuth compression<sup>[7]</sup>. For this reason, the theoretical value of azimuth resolution must be

$$\Delta A = \frac{1}{2} D \quad (3-31)$$

### 3.4 Azimuth Sampling Criteria

SAR is using a train of pulses often with some modulation, where the pulse repetition frequency<sup>[7]</sup> (PRF) is the rate for the emitted pulses. The maximum PRF is set to avoid range ambiguity and the minimum PRF is set by the Doppler content which is given according to:

$$f_d = -\frac{2v \cos \theta_s}{\lambda} \quad (3-32)$$

where  $v$  is the platform velocity,  $\lambda$  is the wavelength and  $\theta_s$  is the angle to the target. The maximum Doppler frequency arises at the greatest angle, which is given by real antenna beamwidth.

The PRF interval is given by:

$$PRF_{\min} \leq PRF \leq PRF_{\max} \quad (3-33)$$

$$PRF_{\min} = 2f_{d \max} \quad (3-34)$$

$$PRF_{\max} = \frac{2R_{\max}}{c} \quad (3-35)$$

where  $R_{\max}$  is the maximum range of the illuminated and  $f_{d \max}$  is the maximum Doppler frequency of a target.

### 3.5 Simulation for Azimuth Processing

As an example, the scenario is showed in Fig. 3-5 and the parameters are listed in table 3-1. The azimuth processing can be achieved as well as that discussed in chapter 2 by using matched filter and the reference signal is

$$s_{ref}(t) = \exp\left[j\pi k_a(t - \tau_a)^2\right] \quad \tau_a - \frac{T_p}{2} \leq t \leq \tau_a + \frac{T_p}{2} \quad (3-36)$$

The  $\tau_a$  is given by

$$\tau_r = \frac{x_{mid}}{v} \quad (3-37)$$

where  $x_{mid}$  is the center distance of target area in azimuth direction.

Fig. 3-5 shows the reference signal and Fig. 3-6 shows the uncompressed echo and the output after azimuth compression.



## Chapter 4 Stripmap SAR Imaging Procedure

SAR usually moves along a straight line with uniform speed. In stripmap SAR, the beam remains at constant squint angle perpendicular to the flight path and continuously observes a strip of terrain parallel to the flight path. The beam is often broadside. If beam is not broadside, we refer to the radar as squint mode SAR.

### 4.1 Raw Data

The analysis of point target that discussed here is only for broadside stripmap SAR. SAR transmits and receives pulses by using fixed PRF during the process of motion. Fig. 4-1 shows the transmitted and received signal sequence in time domain.

In order to do digital signal processing, it is necessary to sample in range direction (fast-time domain). Assume that sampling period is  $T_s$ , then  $t_{end} - t_{start} = M \times T_s$ . As illustrated in Fig. 4-2, if  $N$  pulses is transmitted in azimuth direction (slow-time domain) and there are  $M$  sampling points in range direction, the received signal is composed of the  $M \times N$  data matrix. The  $M \times N$  data is used to called raw data and the data set contains  $M$  range profiles through  $N$  Doppler profiles.

## 4.2 Imaging Procedure

The raw data<sup>[8]</sup> can be observed directly before imaging procedure. In principle, SAR imaging procedure is a two-dimensional correlation process. Thus the most effective method is to do the two-dimensional matched filter to raw data.

Correlation Process of two-dimensional SAR data<sup>[9]</sup> with independent range and azimuth reference signal is illustrated in Fig. 4-3. Here, columns of range response data are transformed into columns of frequency response. Columns of frequency are then multiplied, element by element, by the frequency-domain form of the range reference signal to form columns of frequency-response products. Column-by-column inverse Fourier transforms of these products produce cross-correlated response in the range domain versus time history  $t_r$ . The data have now undergone range compression. Range compressed columns are stored, from azimuth data rows are read out row by row. Azimuth correlation is then carried out in exactly the same way as range correlation, except that it is down in the time-history dimension instead of the range-delay dimension. The final result is the output image frame. The above process is illustrated in terms of a processor block diagram in Fig. 4-4.

### 4.3 Simulation for Point Target

Consider the case that the aircraft moves along the straight line and SAR antenna illuminates a point target. The Parameters are described in detail in Table 4-1.

The real part of raw data is shown in Fig. 4-5. Fig. 4-6 is the result after range compression and range correction. After azimuth compression, Fig. 4-7 shows the SAR image in the end and Fig. 4-8 shows the -4dB contour of SAR image. From the Figs. 4-9 and 4-10, the azimuth and range resolution can be computed as  $\Delta A = 4.7620m$  and  $\Delta R = 5.0032m$  respectively when the relative amplitude is -4dB.

The second case is that the aircraft moves along the straight line and SAR antenna illuminates multiple point targets. The Parameters are described in detail in Table 4-2. The real part of raw data is shown in Fig. 4-11. Fig. 4-12 and 4-13 are the SAR image and -4dB contour respectively.

### 4.4 Compensation with Variable PRF

Due to the presence of atmospheric turbulences airborne SAR raw data may be affected by deviations from an ideal straight line. Most of SAR system are operated with a fixed PRF, the motion introduced by forward velocity variation should be considered<sup>[10]</sup>. It is necessary that phase errors, resulting from spurious platform motion errors, are compensated. The platform motion

error is defined as the error between the actual flight path and the nominal one and is illustrated in Fig. 4-12.

In modern airborne SAR system, the motion compensation can be realized by variable PRF<sup>[11]</sup>, applying a range-depedent phaseshift to each receive pulse and delaying it. By adjusting the PRF, one compensates for the aircraft forward-velocity variations, so that the emissions will occur at constantly spaced intervals. Adjusting the phase and range delay, one compensates for the displacement in line-of-sight (LOS) direction that extracted from the inertial Navigation System (INS) and the Global Position System (GPS). The Fig. 4-15 illustrated the difference between fixed and variable PRF.

Consider the scenery shown in Fig. 4-16 and is illuminated by SAR. The parameters are described in detail in Table 4-3. Fig. 4-17 shows the actual and nominal flight path. Fig. 4-18 and 4-19 show the range compressed image and final SAR image with nominal flight path respectively. Fig. 4-20 shows the final SAR image with actual flight path. Because of the LOS phase error, the image is worse than that with nominal path. After compensating the LOS error the final image is shown in Fig. 4-21. Obviously, it is similar to the image with nominal path.

## Chapter 5 Conclusion

The radar can be used for not only detection of the target but also imaging it. SAR technique makes the target imaging possible. The Imaging Procedure is discussed in this paper. From Chapter 2 and Chapter 3, the principle of range and azimuth processing can be realized step by step. Through the simulation, it can be known that the resolution computed from image is similar to the theoretical value. Hence the procedure is correct and it can be used to analyze the relationship between trajectory and resolution.



## Reference

- [1] Bassem R. Mahafza, Ph.D., “Radar Systems Analysis and Design Using MATLAB,” Chapman & Hall/CRC, 2000.
- [2] Byron Edde, “Radar Principles, Technology, Application,” Prentice-Hall International, Inc, 2002.
- [3] Nadav Levanon, and Eli Mozeson, “Radar Signals,” A John Wiley & Sons, Inc, 2004.
- [4] Bassem R. Mahafza, Atef Z. Elsherbeni, “MATLAB Simulations for Radar Systems Design,” Chapman & Hall/CRC, 2004.
- [5] Mehrdad Soumekh, “Synthetic Aperture Radar Signal Processing,” John Wiley & Sons, Inc, 1999.
- [6] 向敬成, 張明友, “雷達系統,” 五南, 2004.
- [7] Robert Ericsson, “Stripmap Mode Synthetic Aperture Radar Imaging with Motion Compensation,” KTH signals sensors and systems, 2005.
- [8] Giorgio Franceschetti, Riccardo Lanari, “Synthetic Aperture Radar Processing,” CRC Press LCC, 1999.
- [9] Donald R. Wehner, “High Resolution Radar,” Artech House, Inc, 2004.
- [10] Yanping Li, Mengdao Xing, Zheng Bao, “A new method of motion error extraction from radar raw data for SAR motion compensation,” IEEE, 2006.
- [11] Joao R. Moreira, “A new method of aircraft motion error extraction from Radar raw data for real time motion compensation,” IEEE Trans. Geosci. Remote Sensing, vol. 28, No. 4, July 1990.

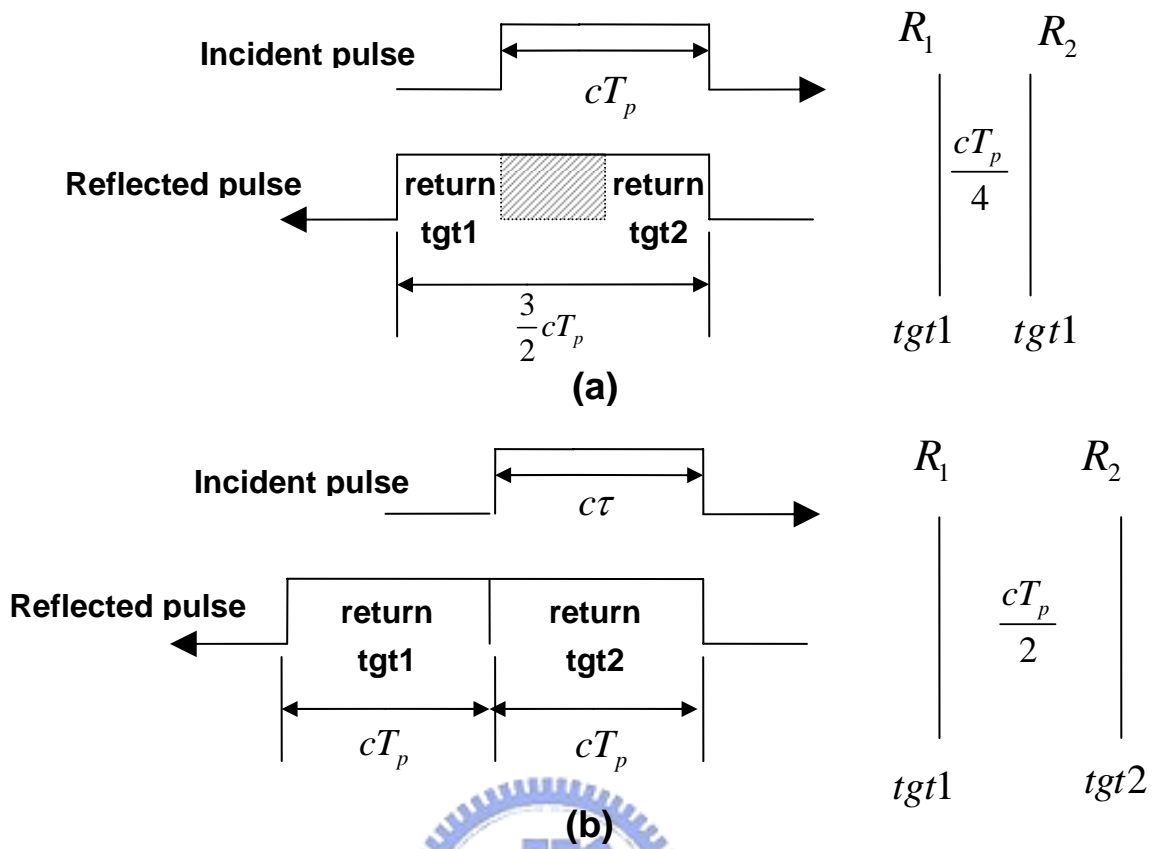


Figure 2-1 (a) Two unresolved targets. (b) Two resolved targets.

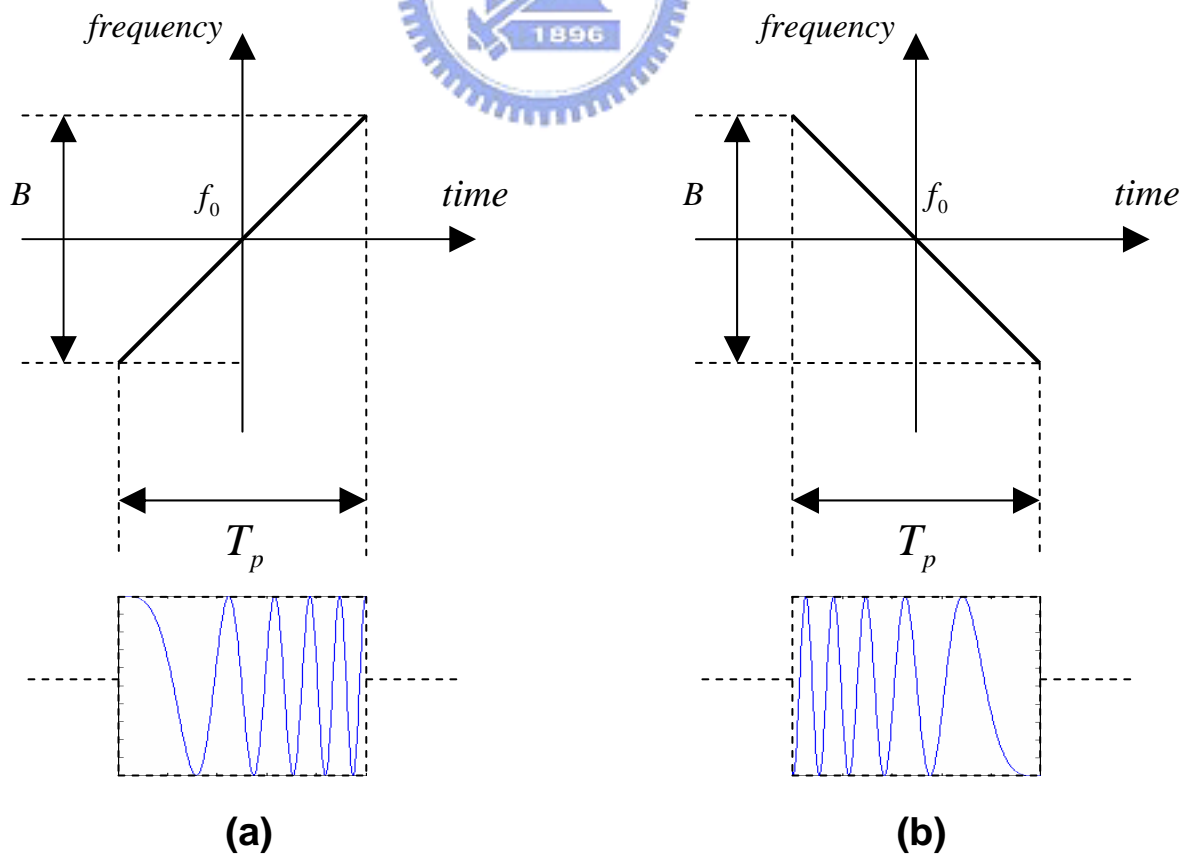
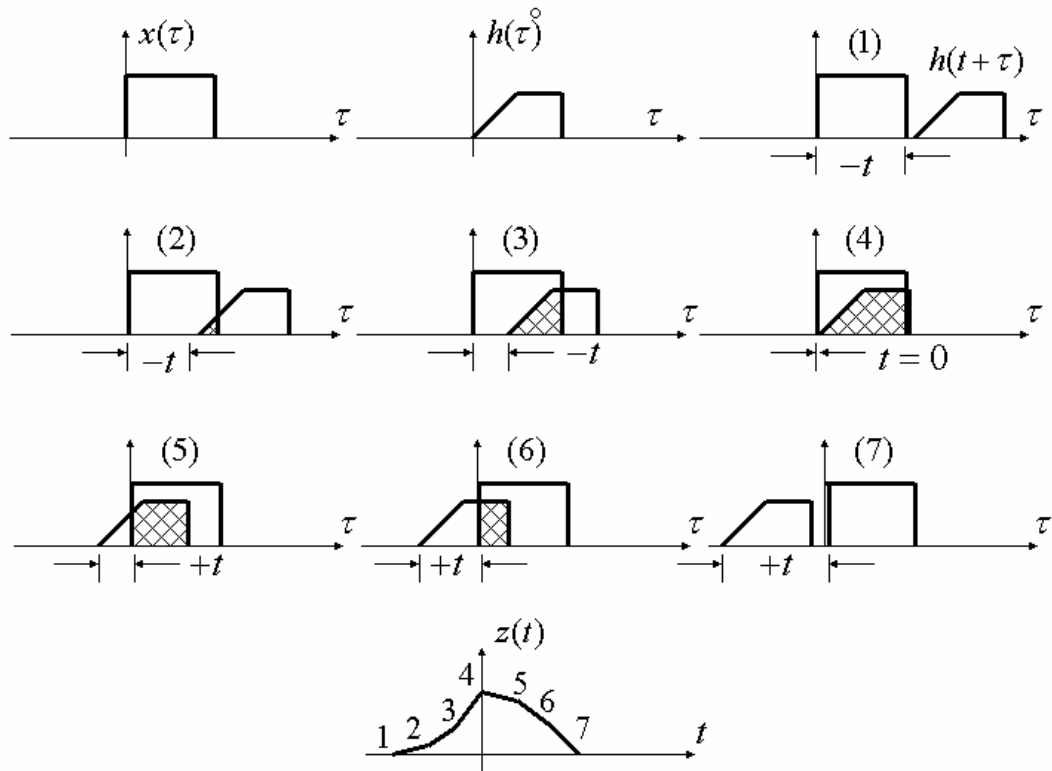
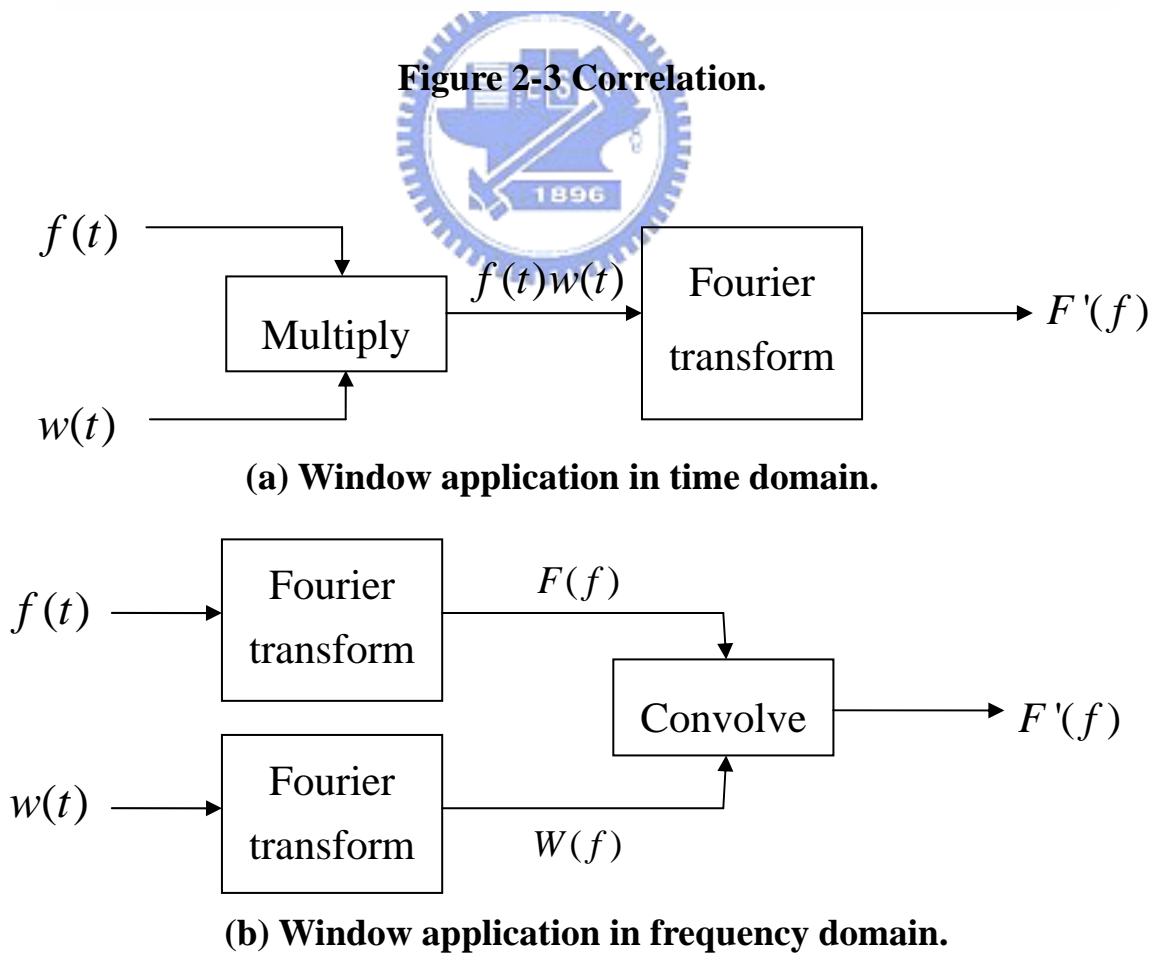


Figure 2-2 Typical LFM waveforms. (a) up-chirp; (b) down-chirp.

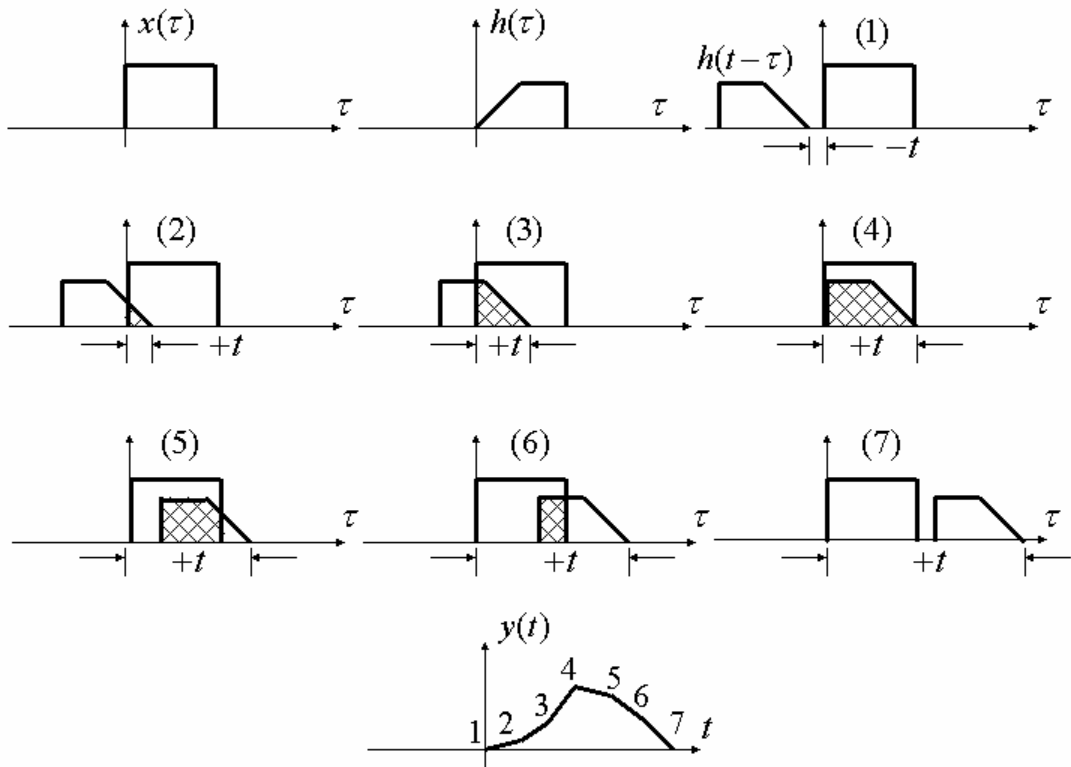


**Figure 2-3 Correlation.**

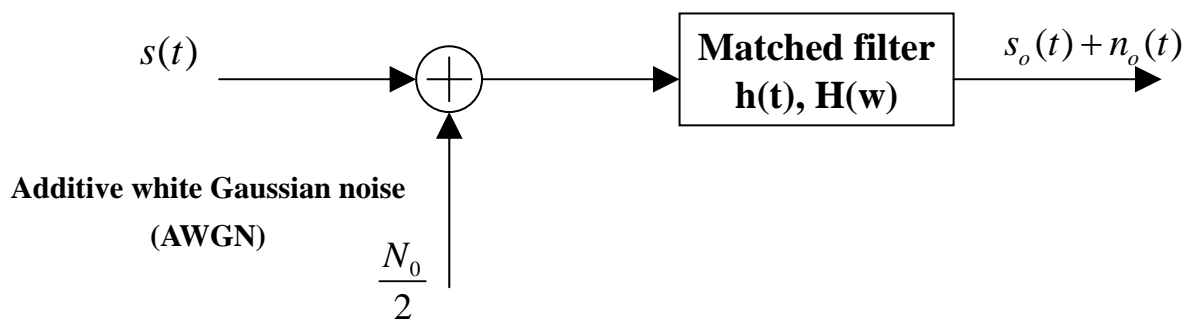
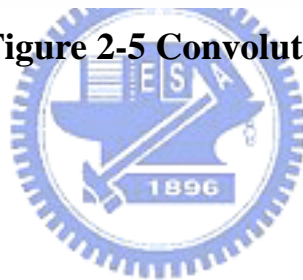


**Figure 2-4 Relationship between Multiplication and Convolution.**





**Figure 2-5 Convolution.**



**Figure 2-6 Matched filter definitions.**

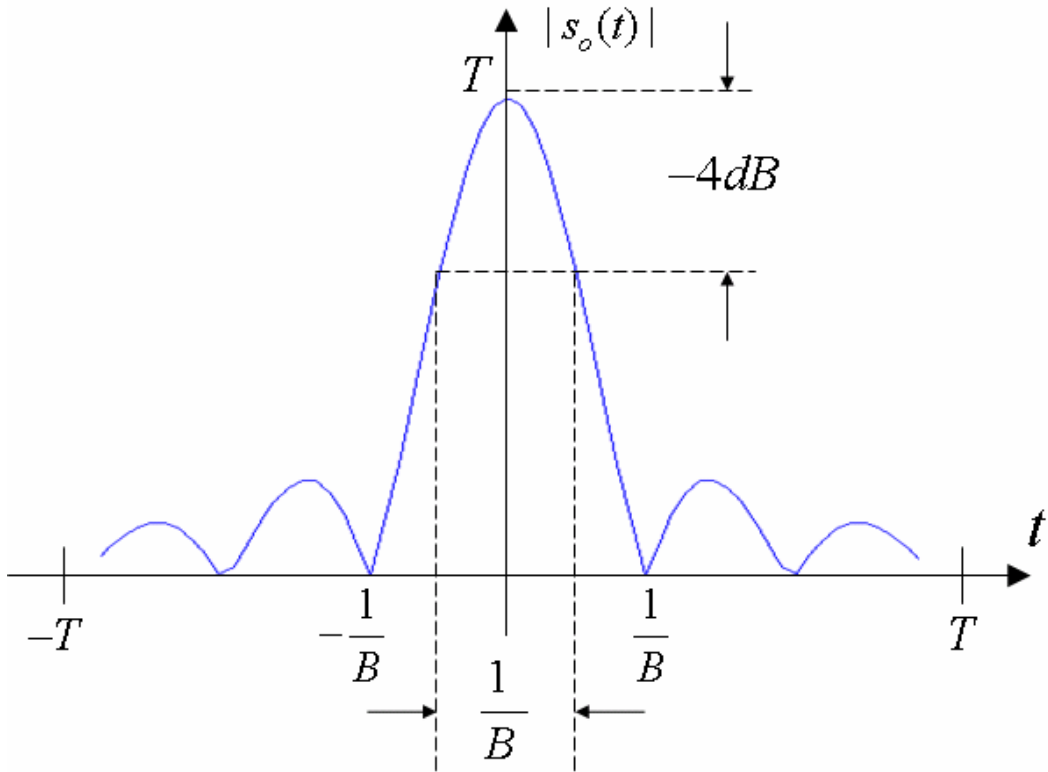


Figure 2-7 Ideal LFM pulse compression.

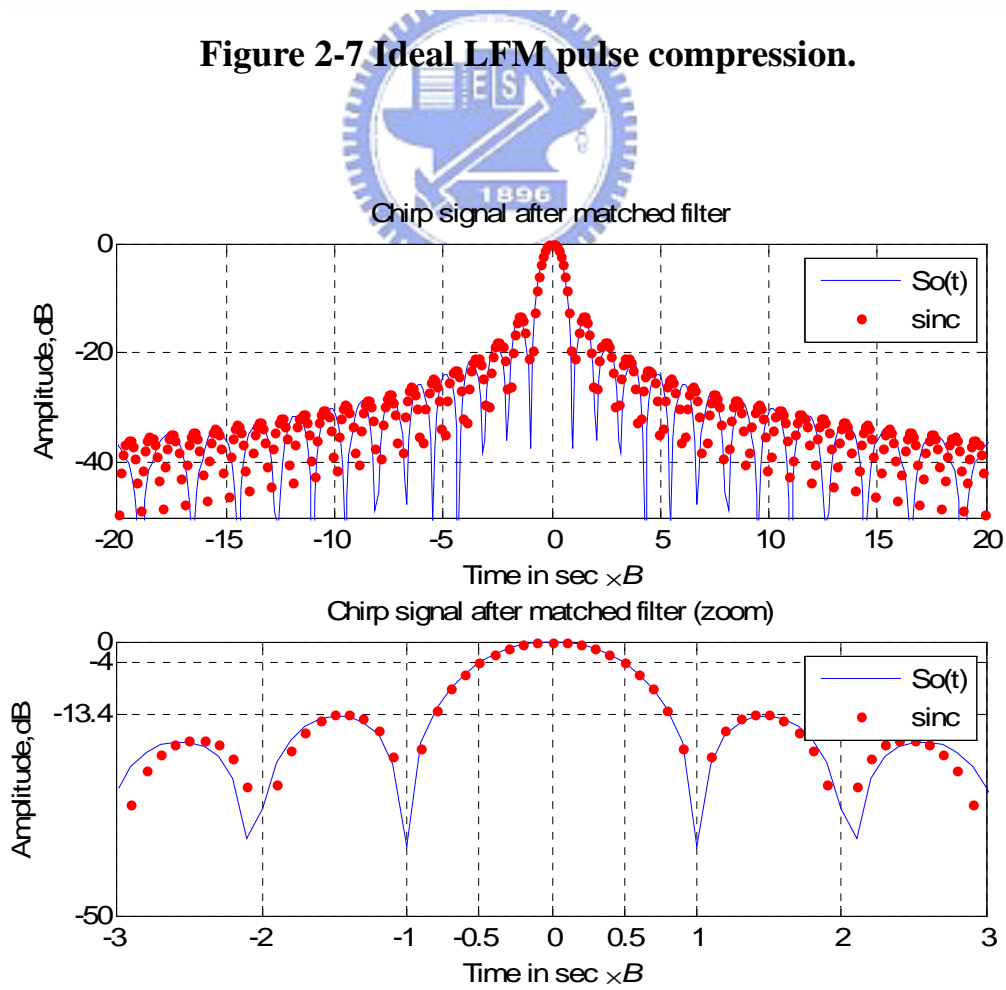
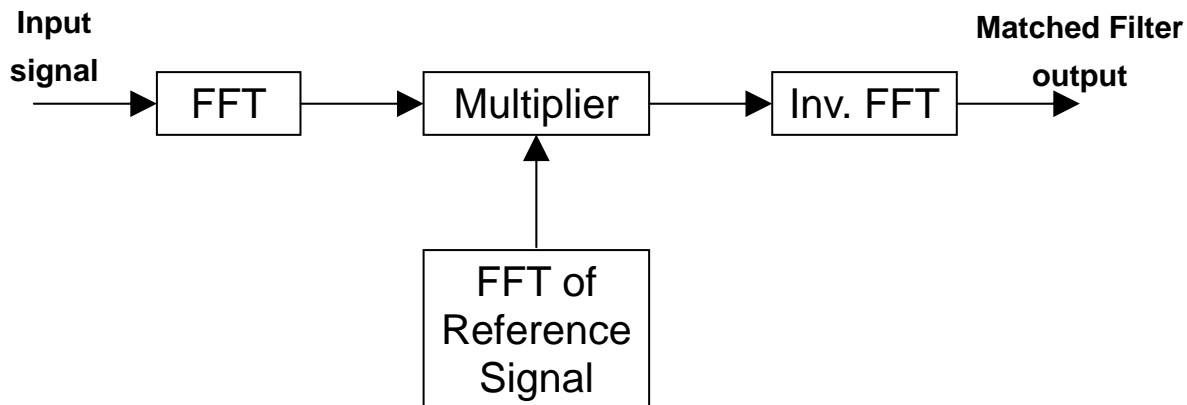
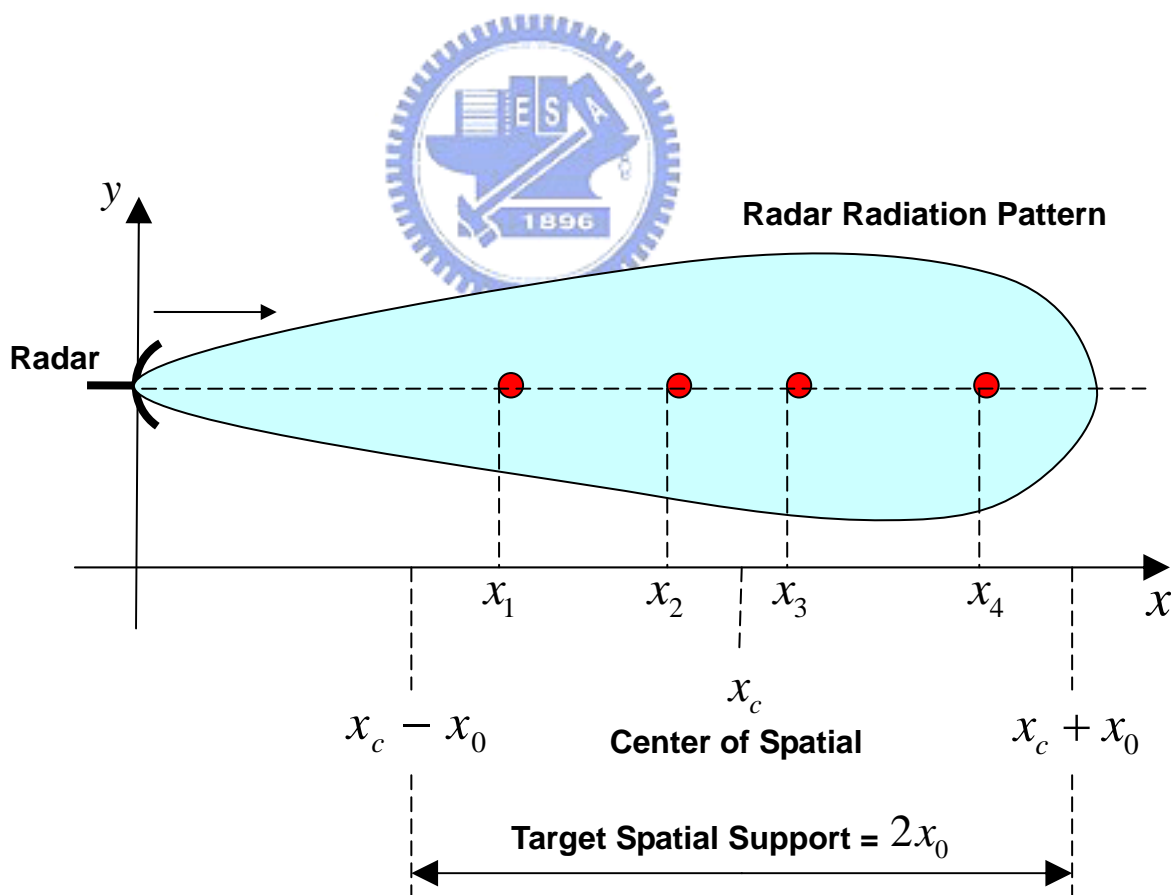


Figure 2-8 LFM pulse after matched filter.



**Figure 2-9** Computing the matched filter output using an FFT



**Figure 2-10** System geometry for range imaging.

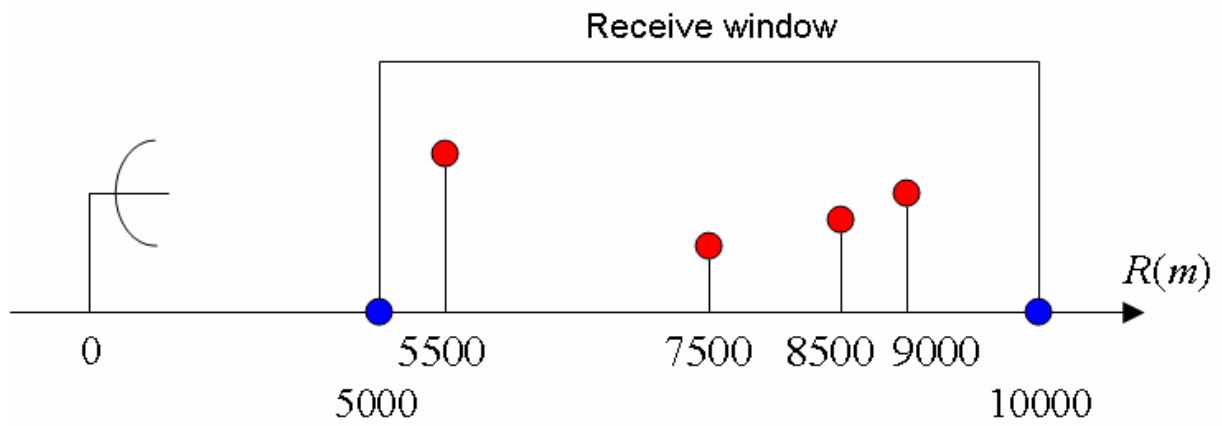


Figure 2-11 Scenery of example in range processing.

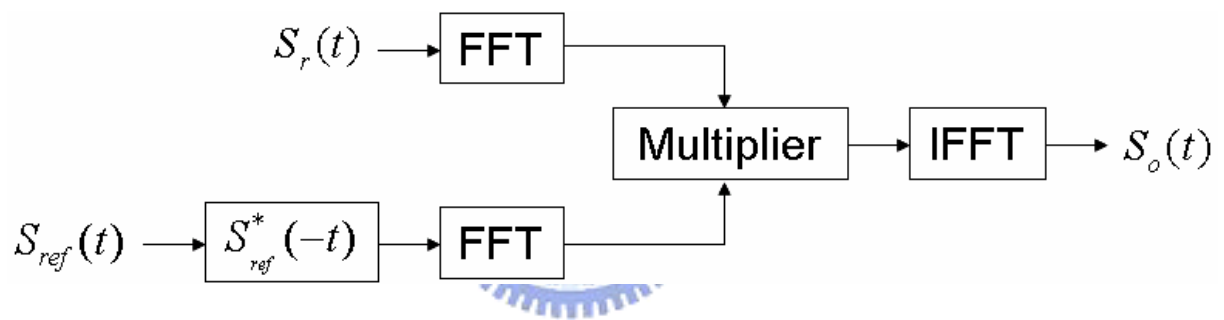


Figure 2-12 First method of range processing.

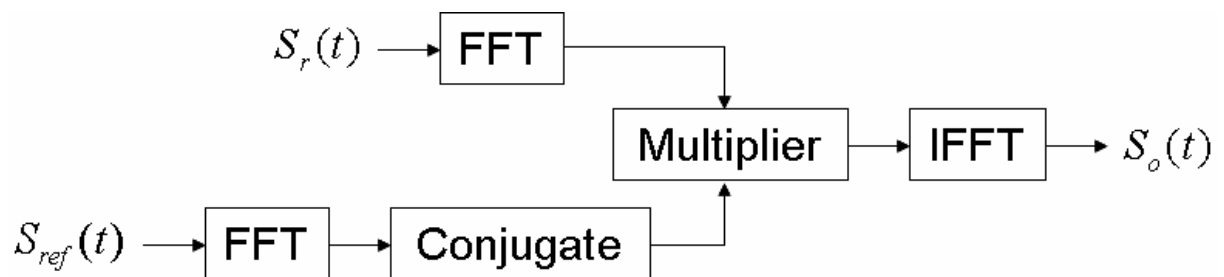
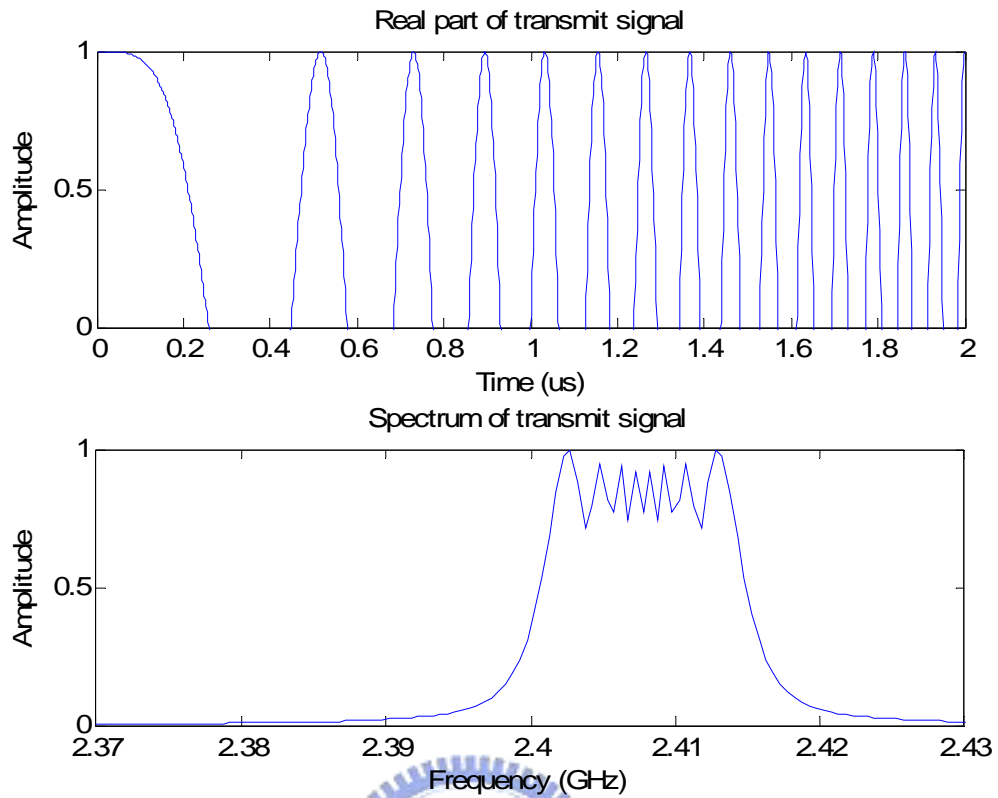
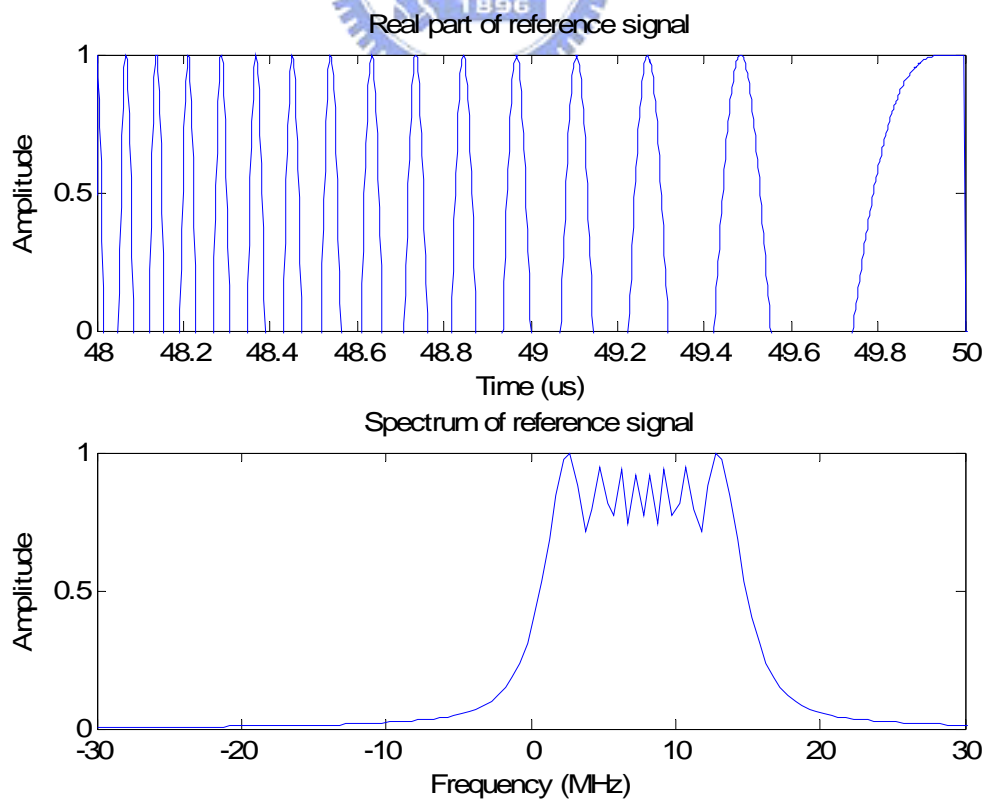


Figure 2-13 Second method of range processing.



**Figure 2-14 Real part and spectrum of transmit signal.**



**Figure 2-15 Real part and spectrum of reference signal.**

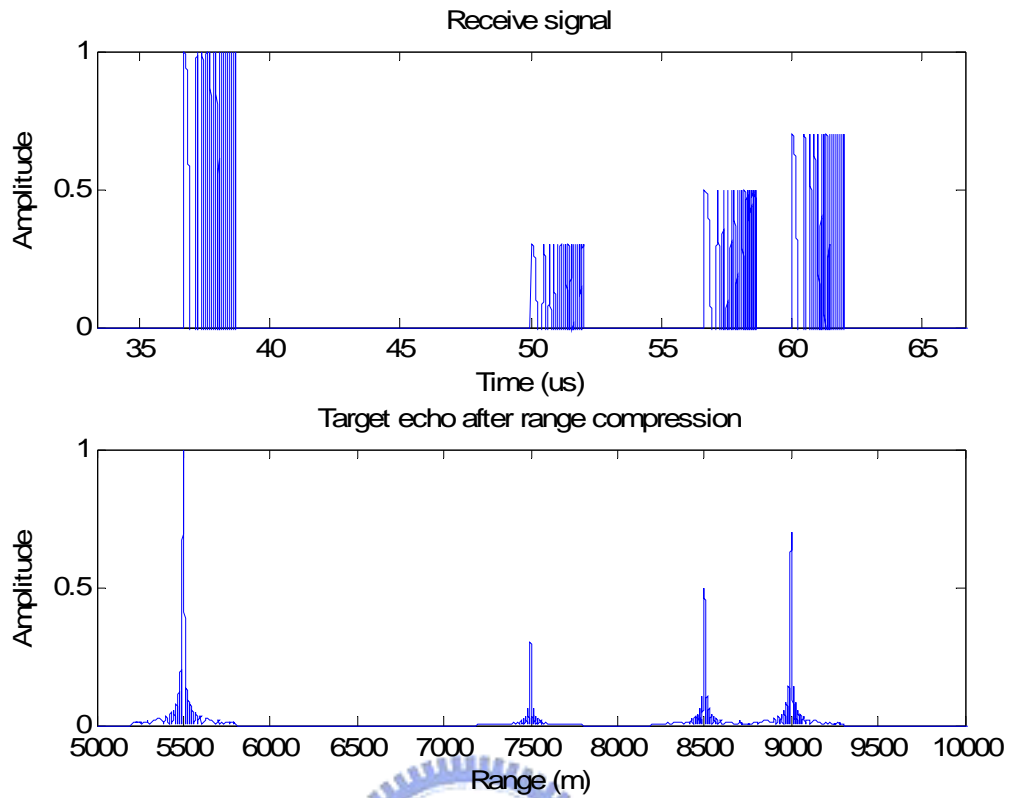


Figure 2-16 Receive signal and Compressed echo signal.

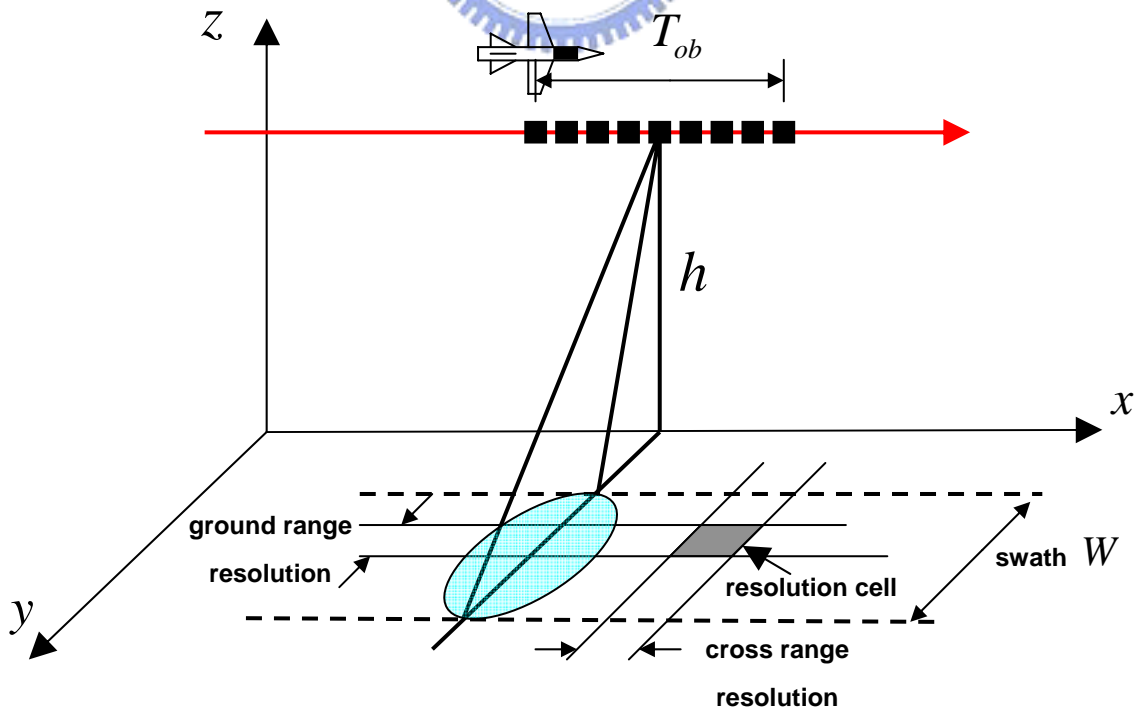


Figure 3-1 Application of airborne Range-Doppler radar.

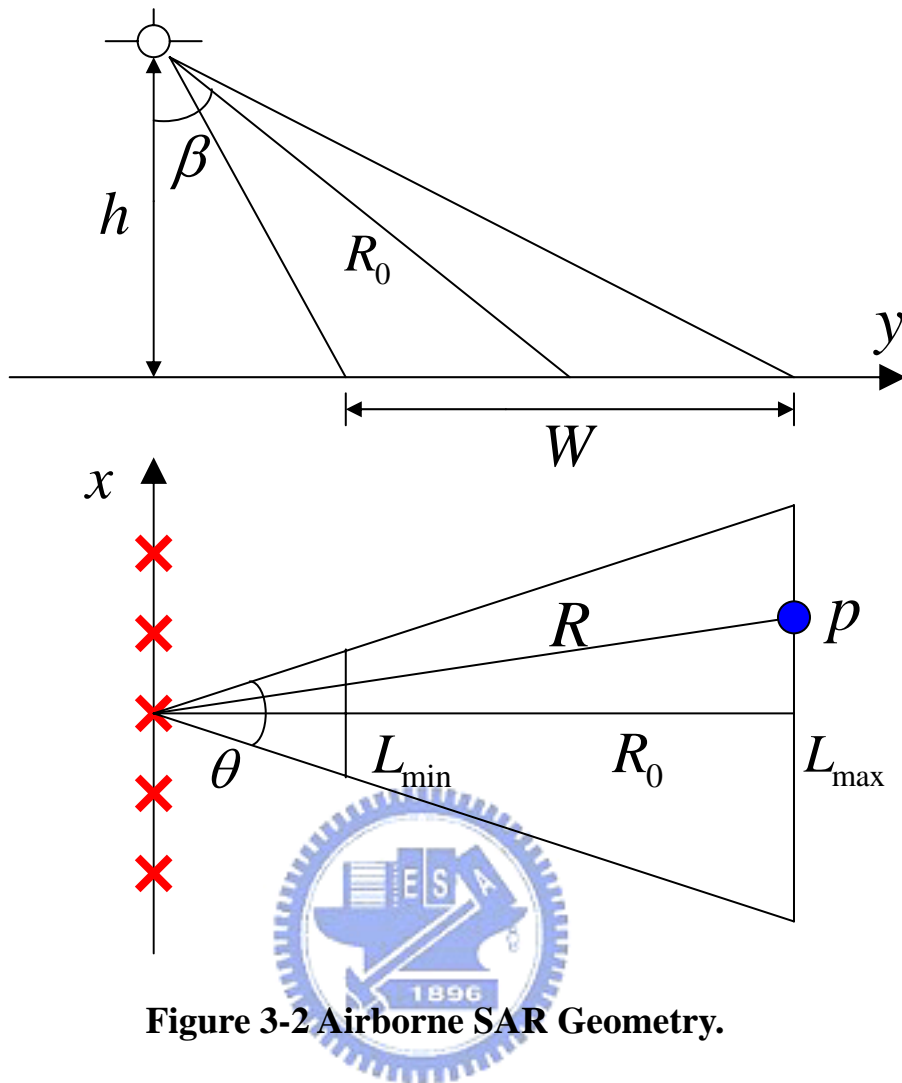


Figure 3-2 Airborne SAR Geometry.

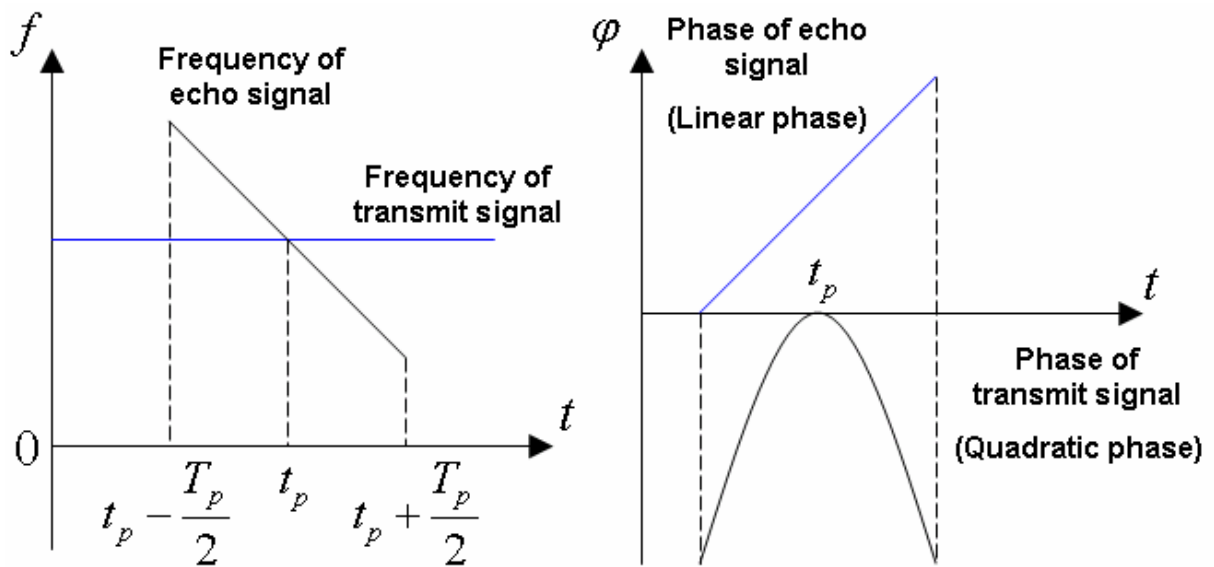
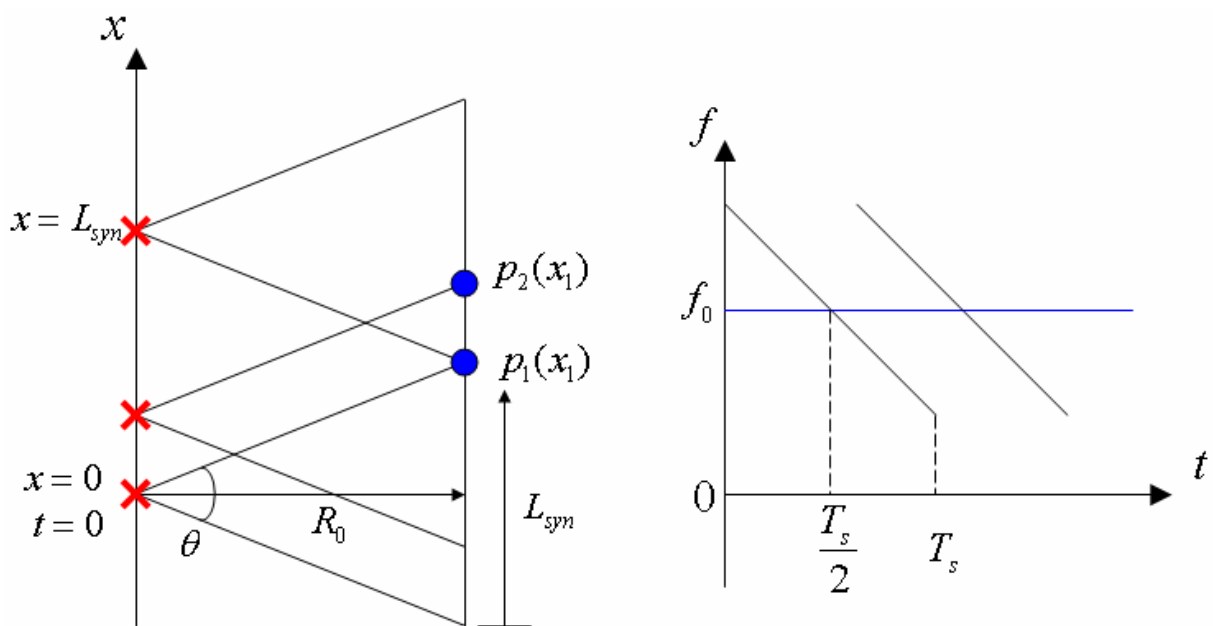
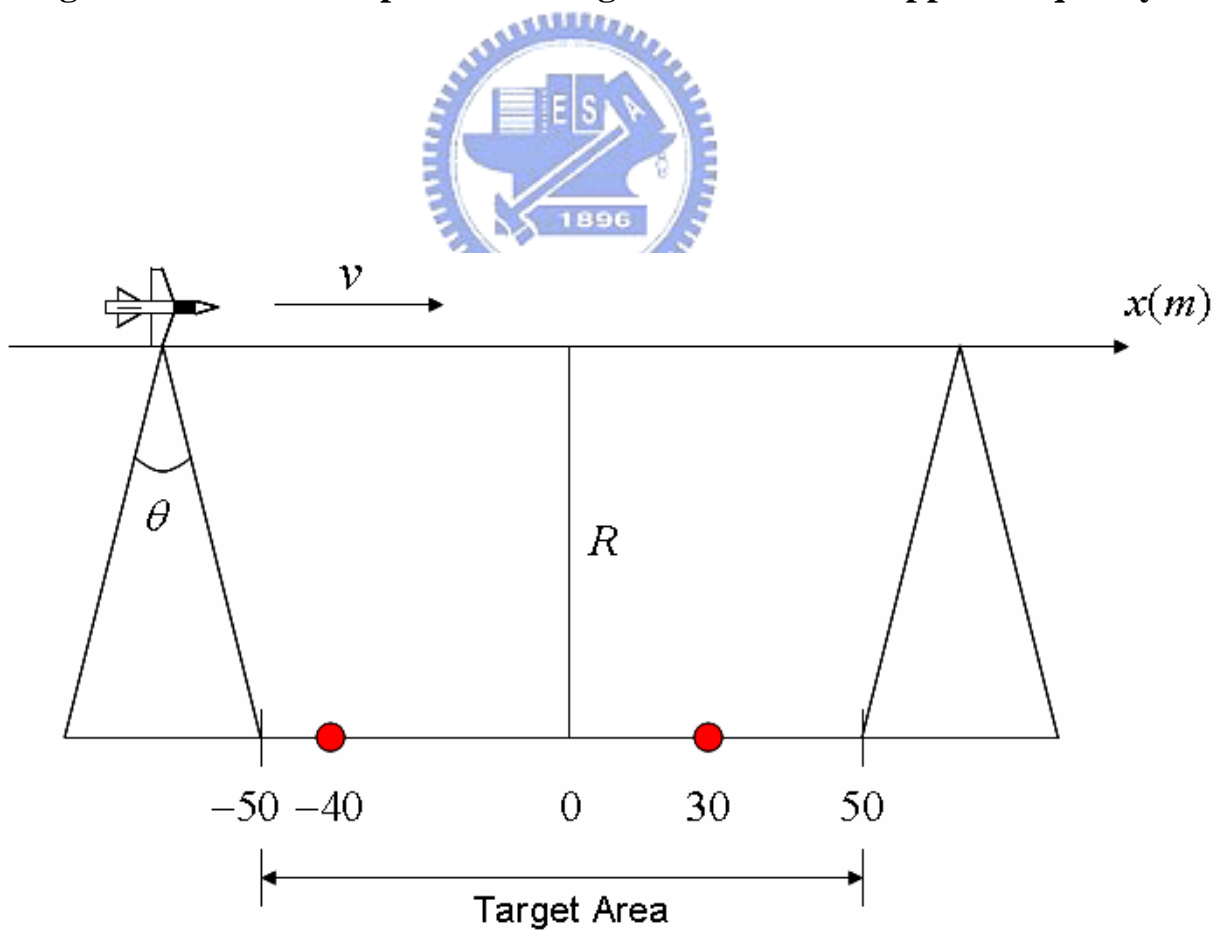


Figure 3-3 Properties of frequency and phase between transmit signal and echo signal.

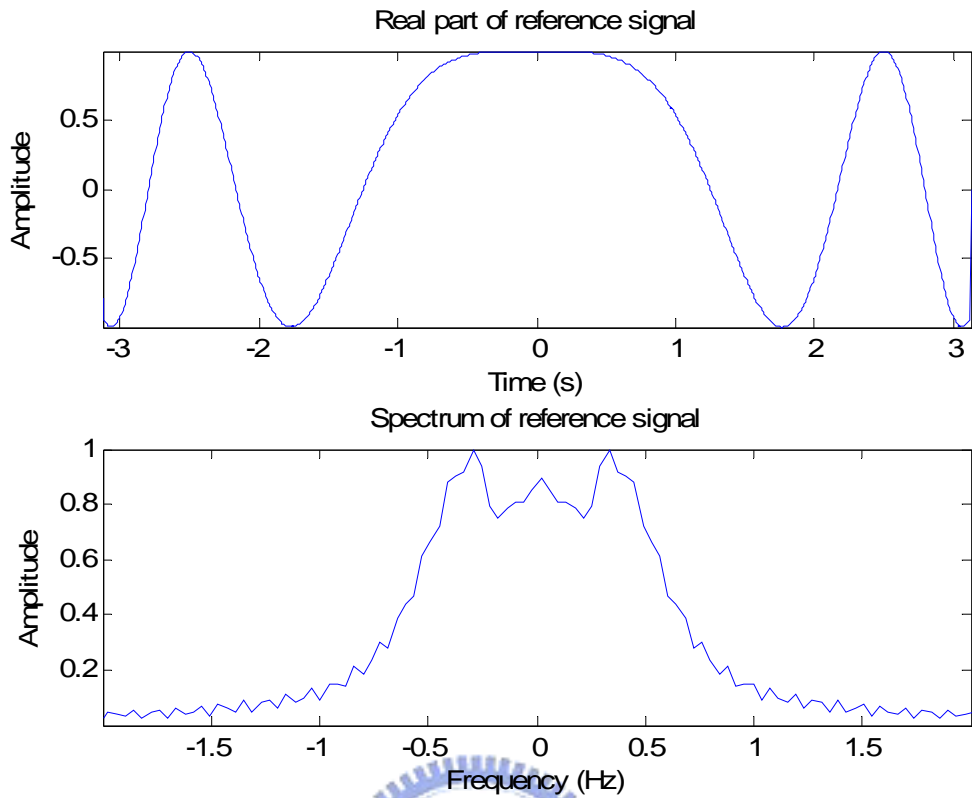


**Figure 3-4 Relationship between target location and Doppler frequency.**

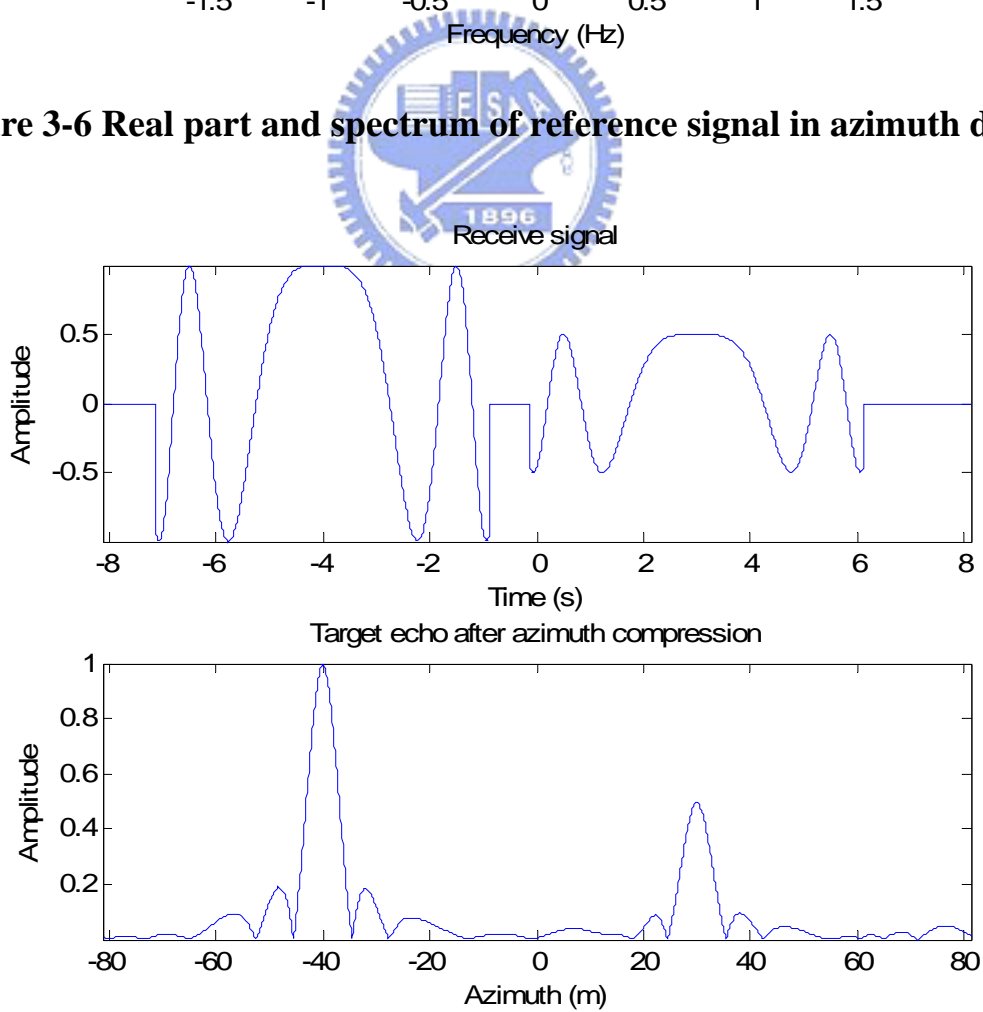


**Figure 3-5 Scenery of example in azimuth processing.**





**Figure 3-6 Real part and spectrum of reference signal in azimuth direction.**



**Figure 3-7 Receive signal and compressed signal in azimuth direction.**

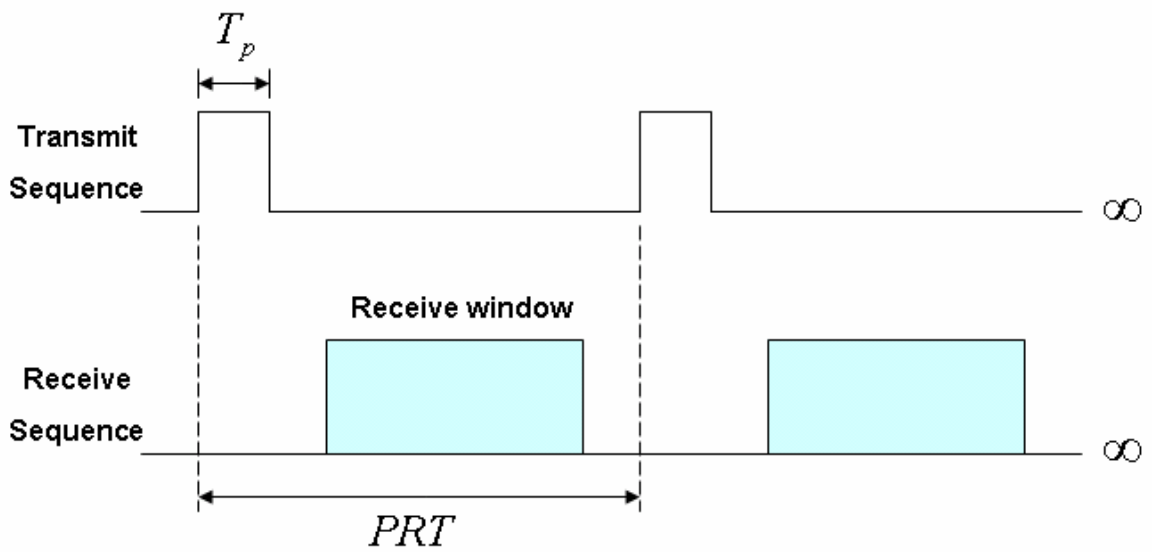


Figure 4-1 Transmitted and received signal in Range-Doppler radar.

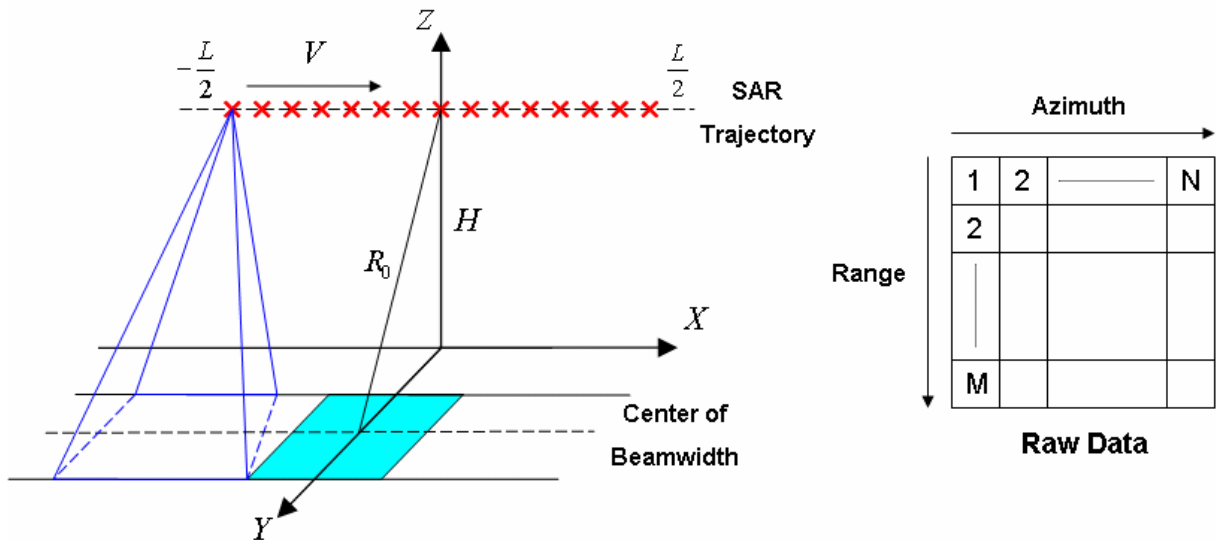


Figure 4-2 The diagram of raw data.

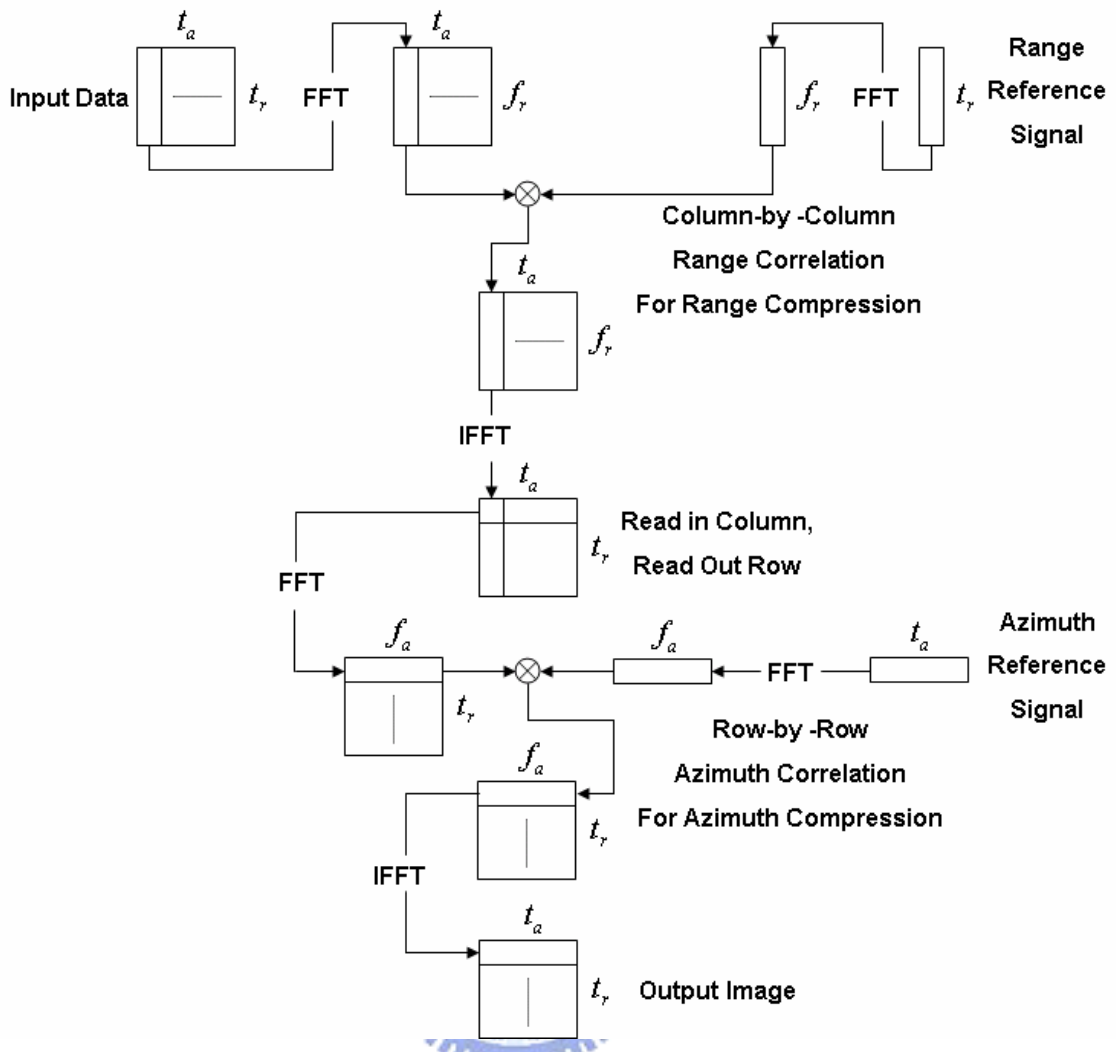


Figure 4-3 Fast correlation with one-dimensional reference signal.

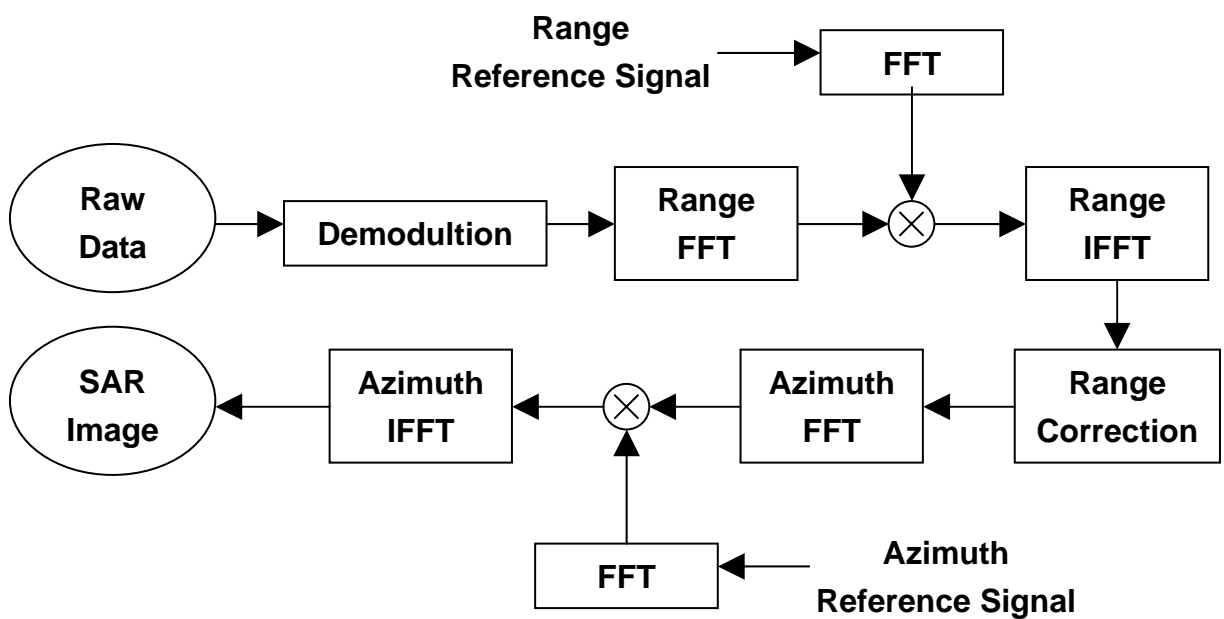
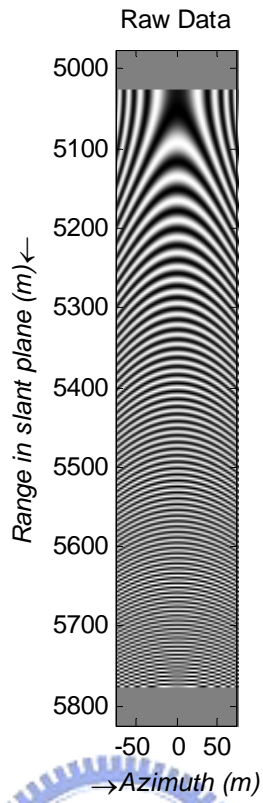
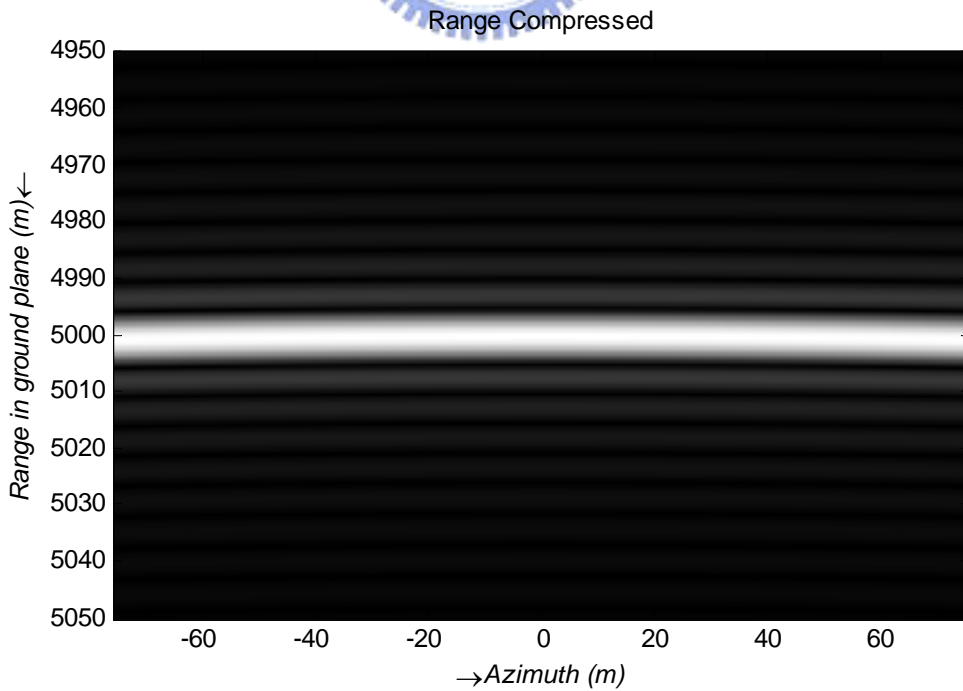


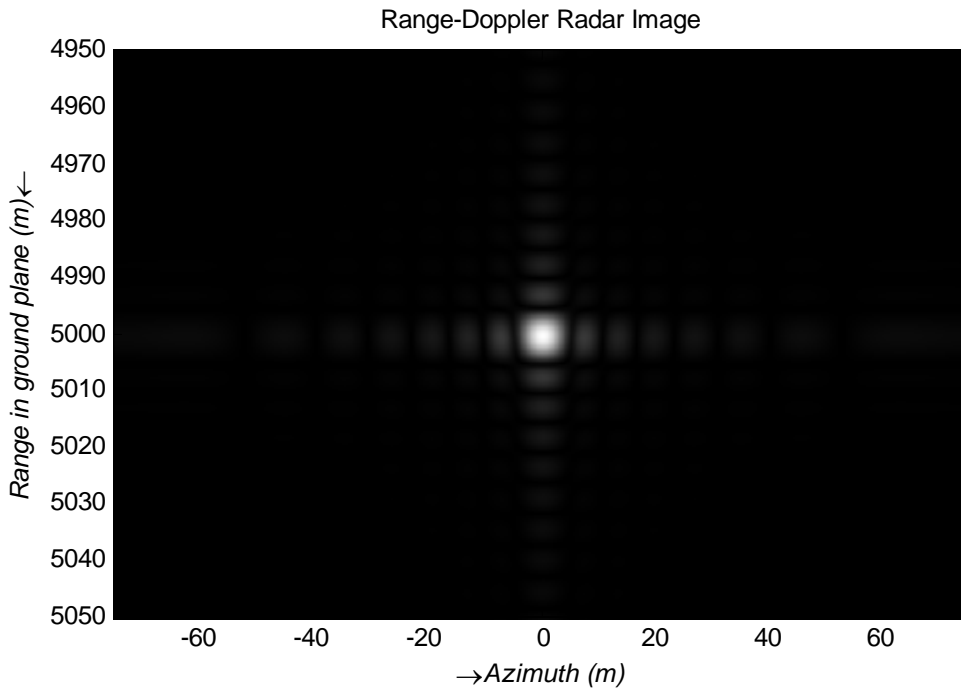
Figure 4-4 Range-Doppler radar imaging procedure.



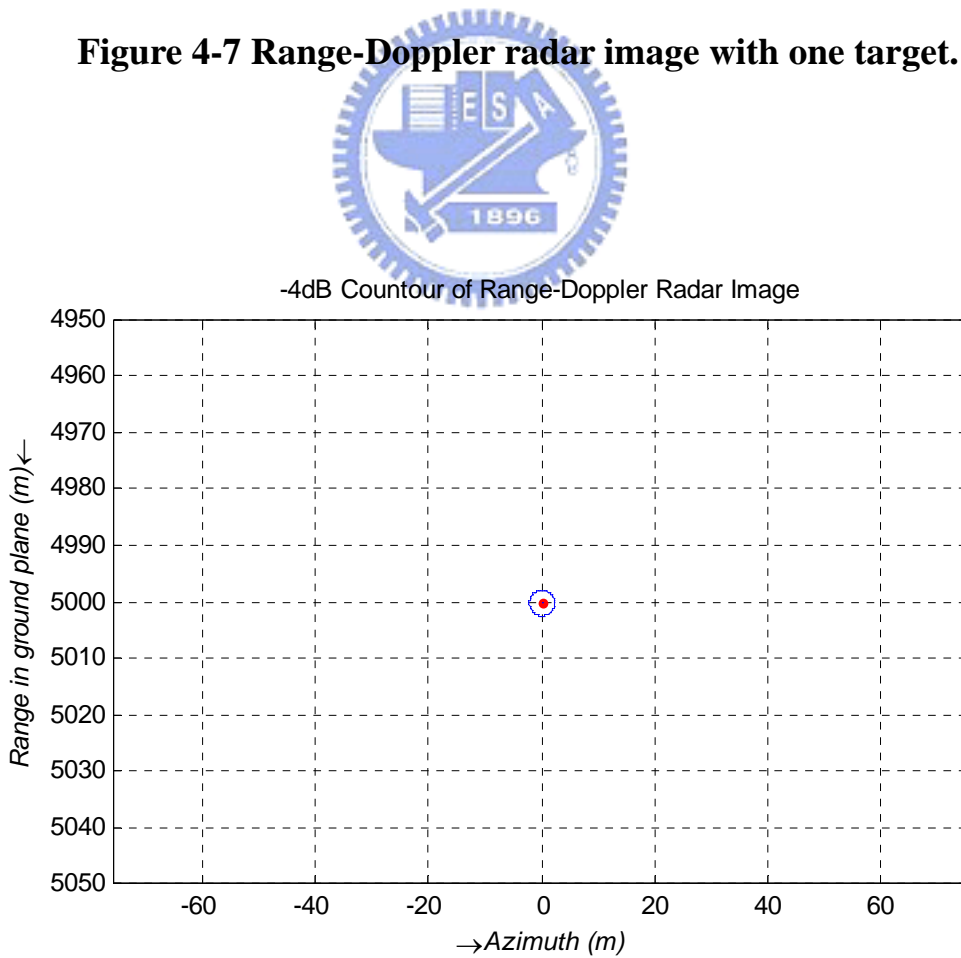
**Figure 4-5 Raw data with one point target.**



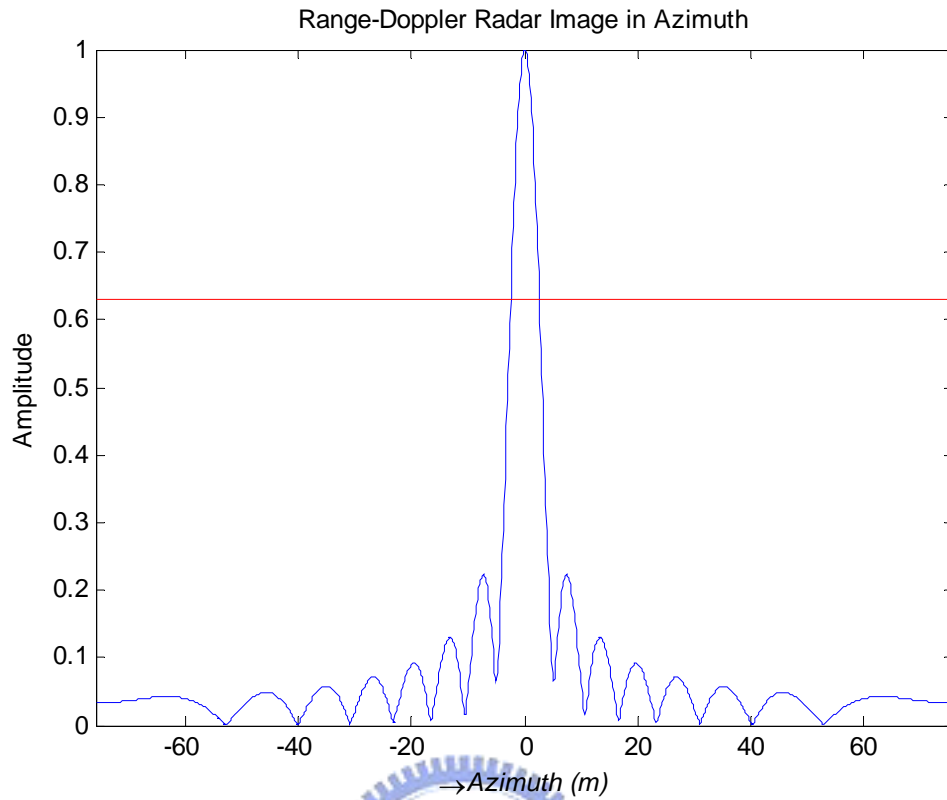
**Figure 4-6 Raw data after range compression.**



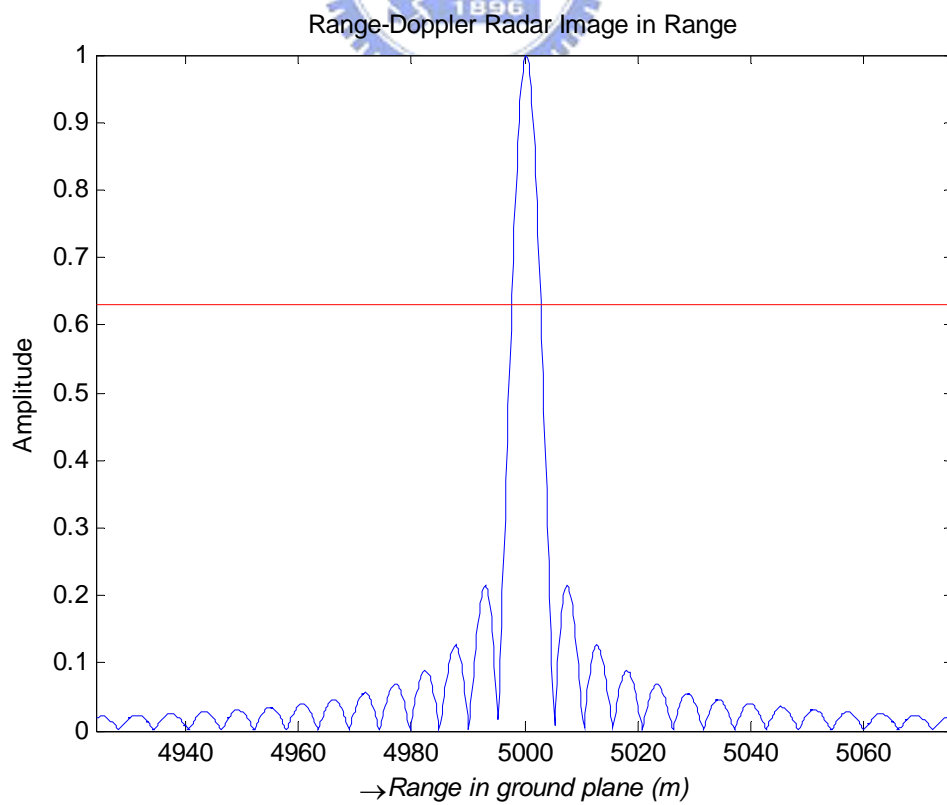
**Figure 4-7 Range-Doppler radar image with one target.**



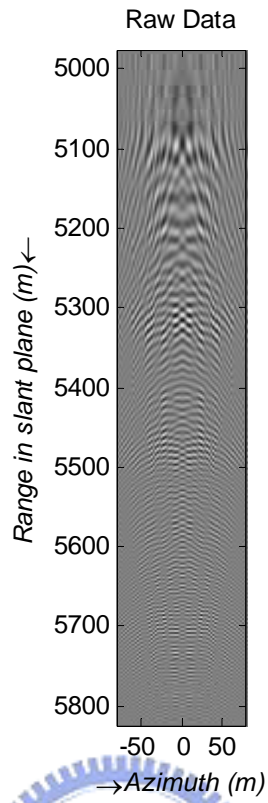
**Figure 4-8 -4bd Contour of Range-Doppler radar image with one target.**



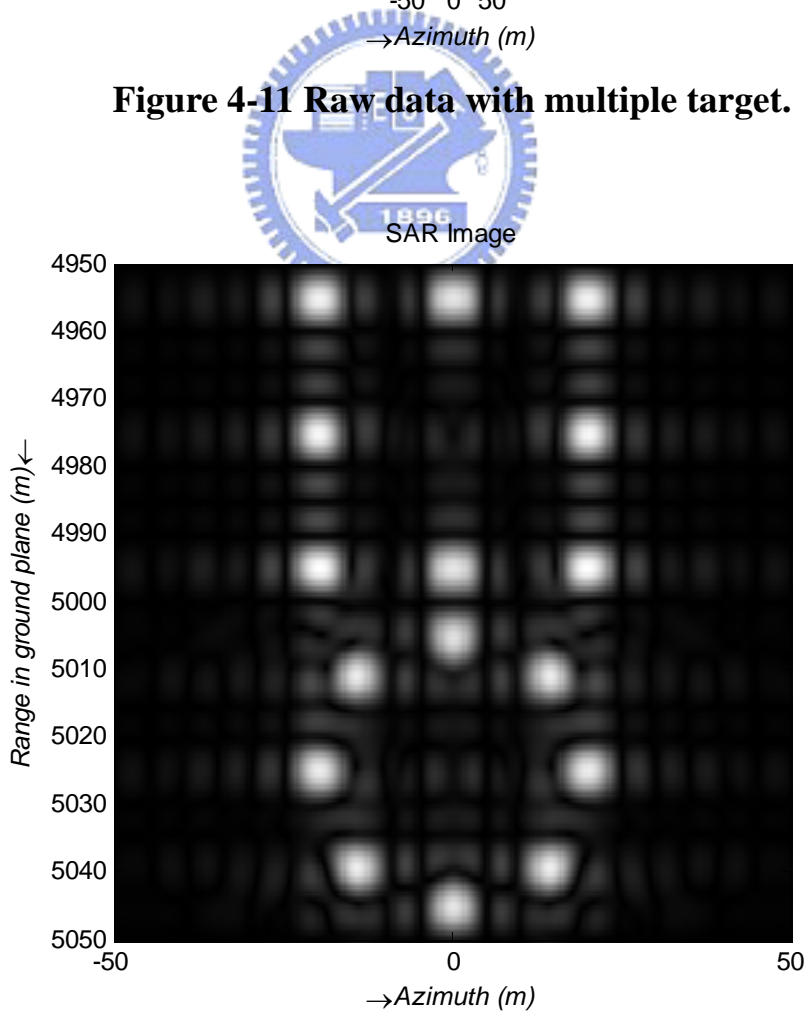
**Figure 4-9 Range-Doppler radar image in azimuth direction.**



**Figure 4-10 Range-Doppler radar image in ground range.**



**Figure 4-11 Raw data with multiple target.**



**Figure 4-12 Range-Doppler radar image with multiple target.**

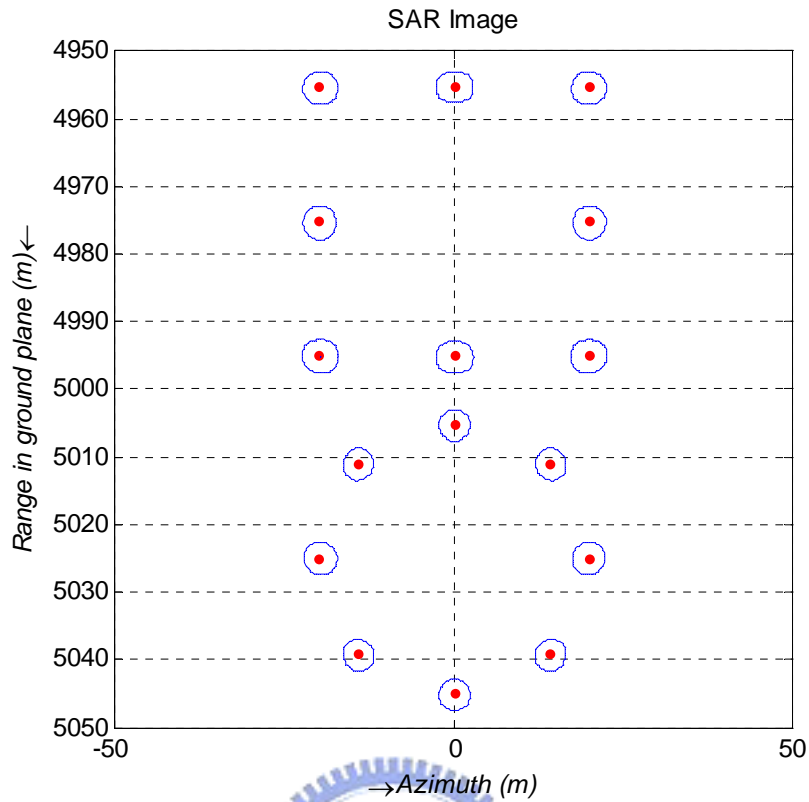


Figure 4-13 -4dB Contour of Range-Doppler radar image with multiple target.

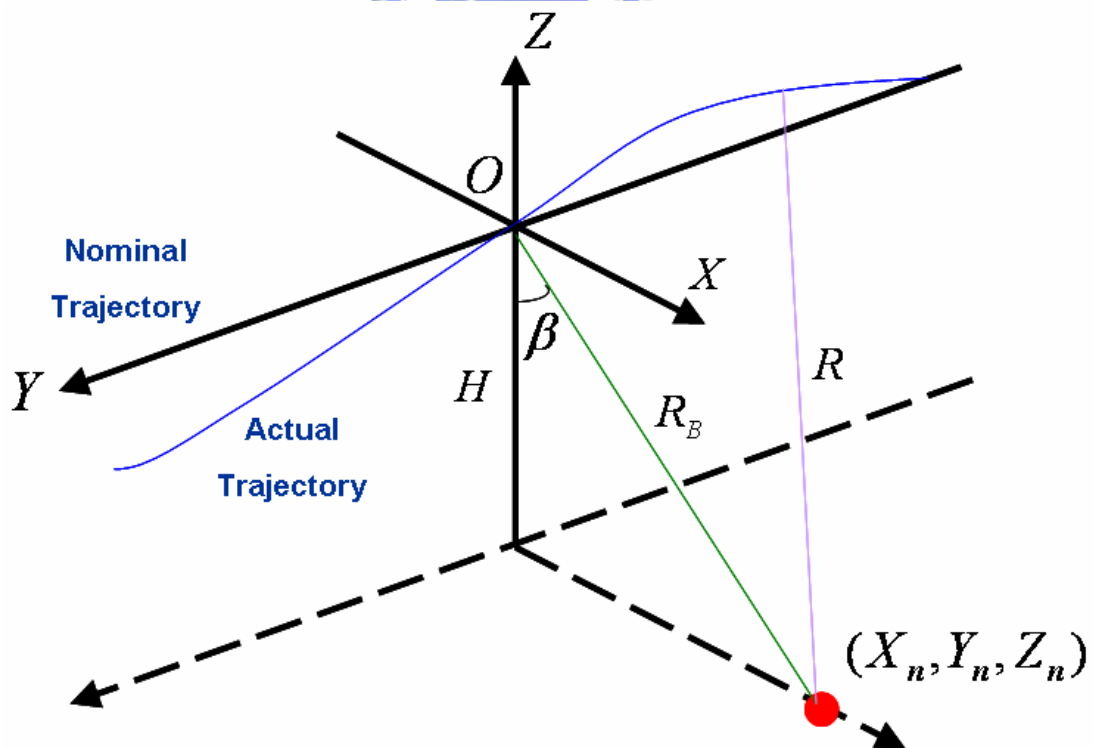
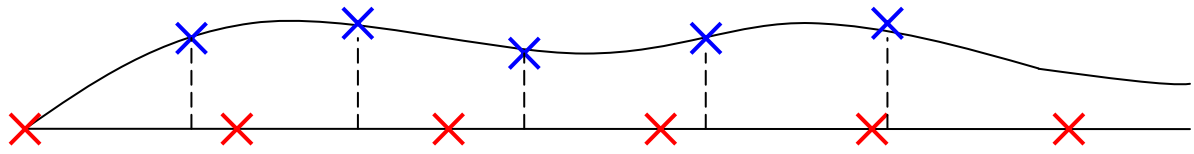


Figure 4-14 The motion error between actual and nominal trajectory.



### Fixed PRF



### Variable PRF

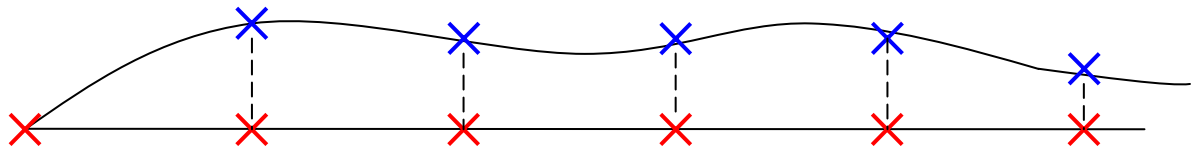


Figure 4-15 The diagram of fixed PRF and variable PRF.

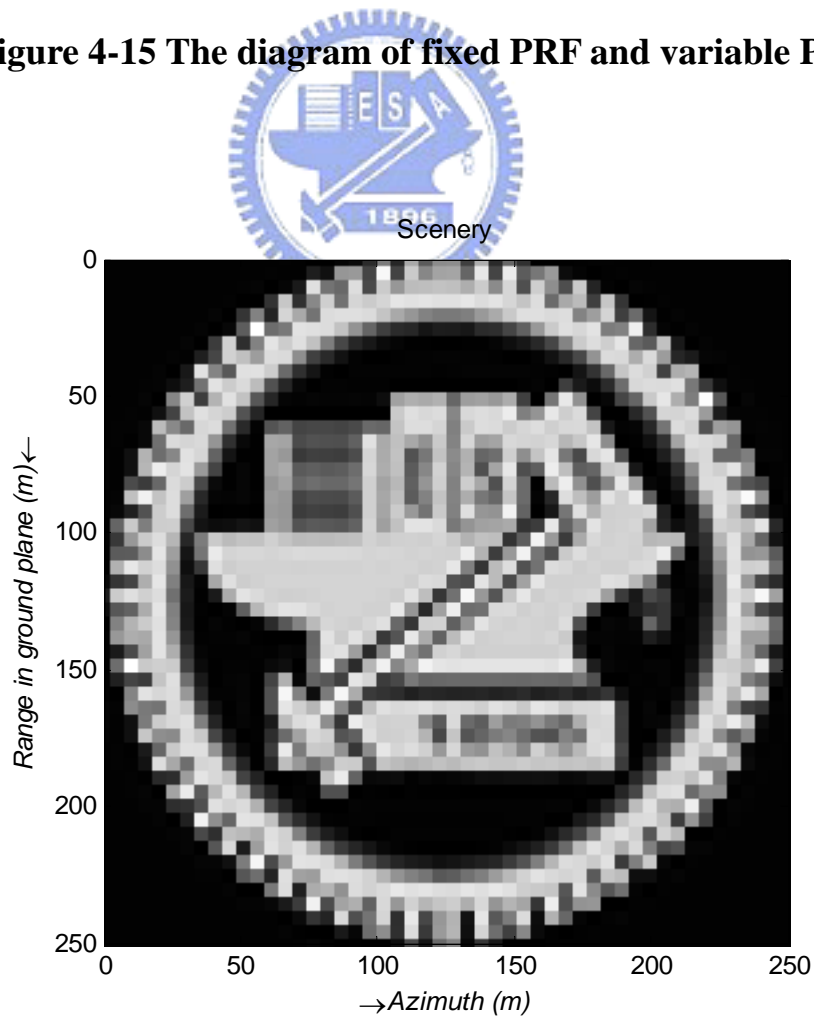
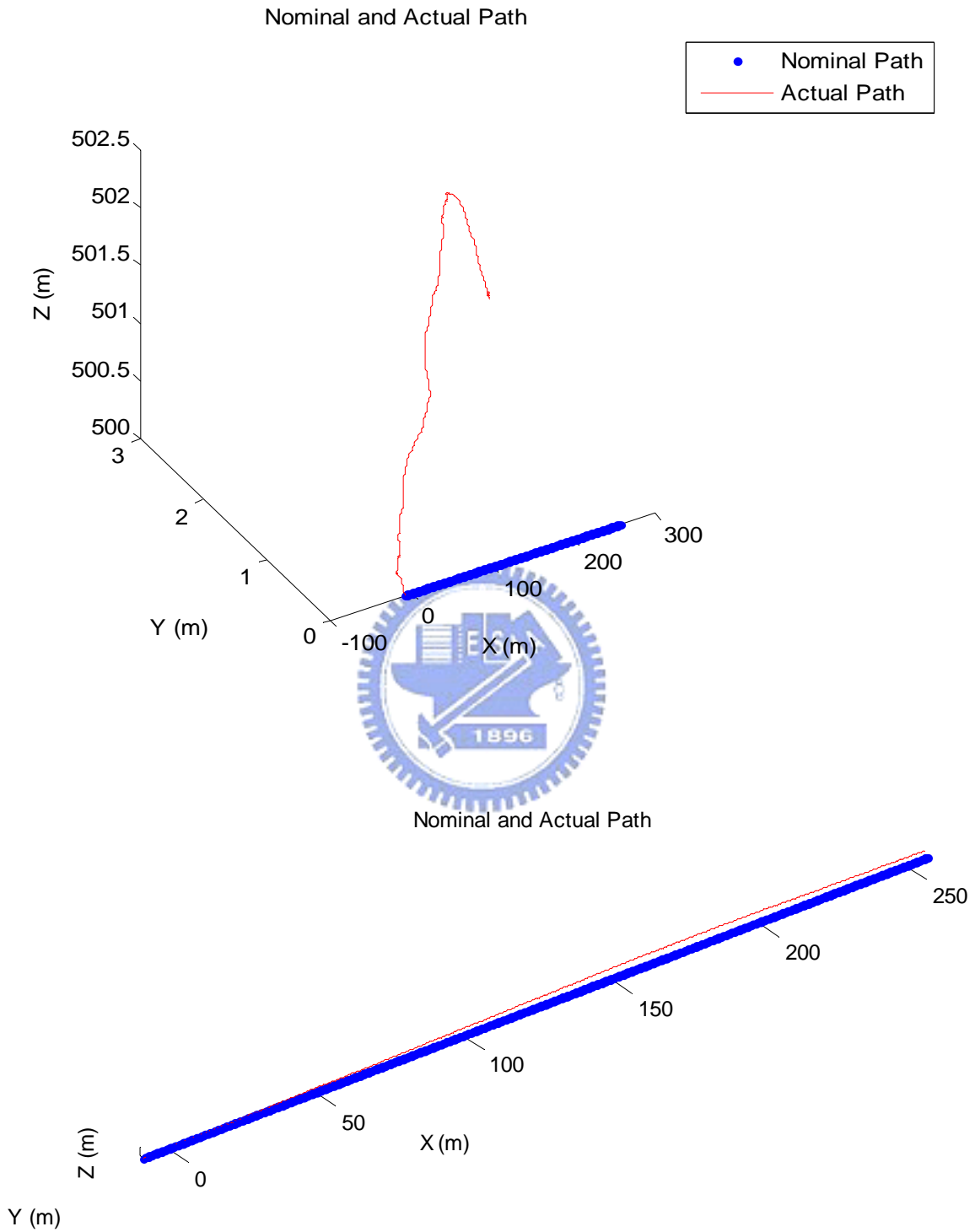
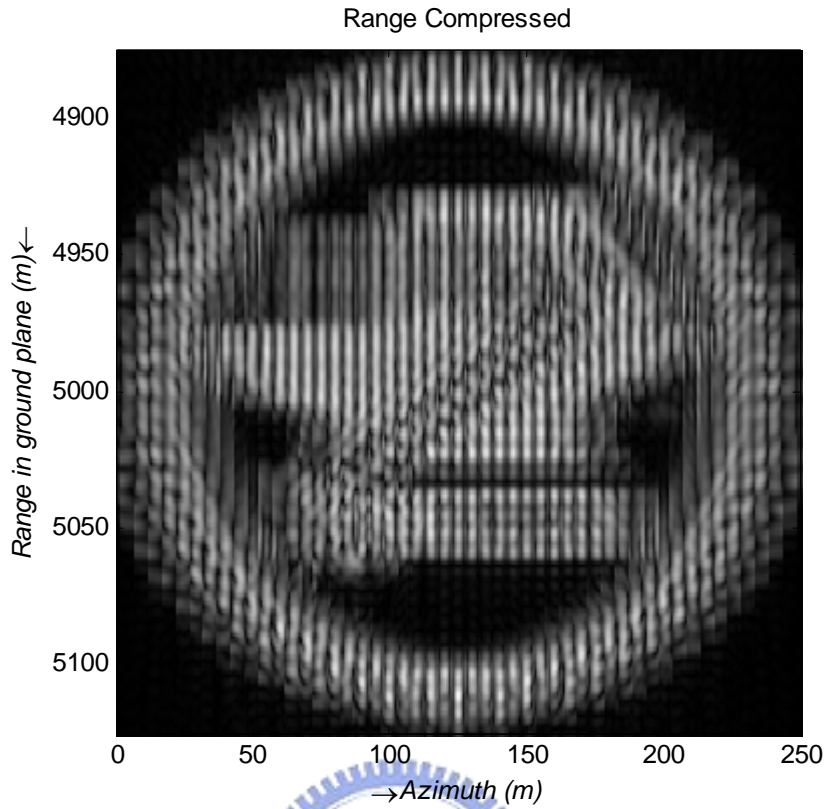


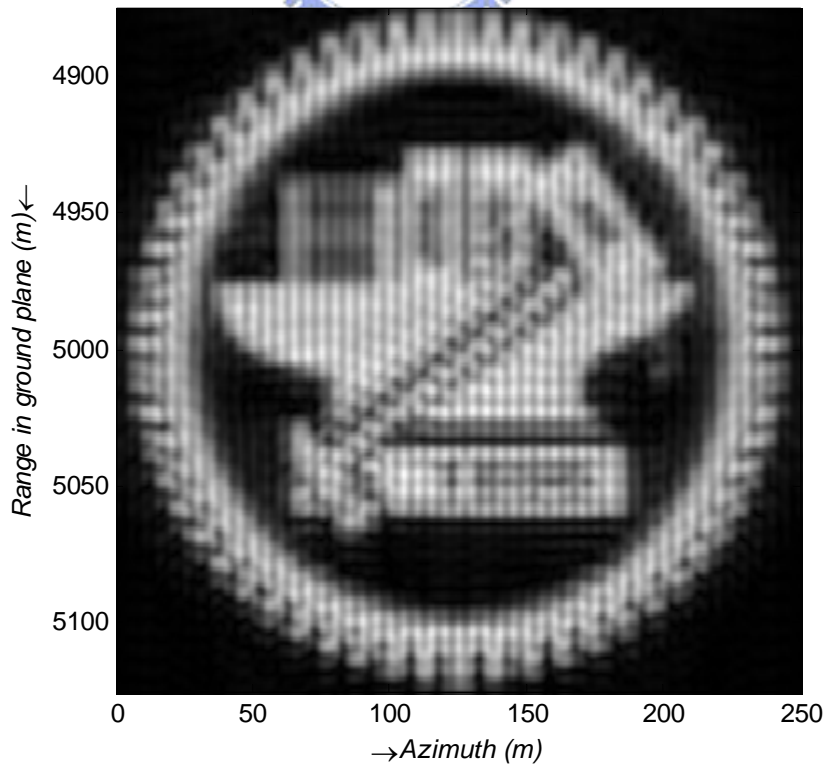
Figure 4-16 The Scenery illuminated by Range-Doppler radar.



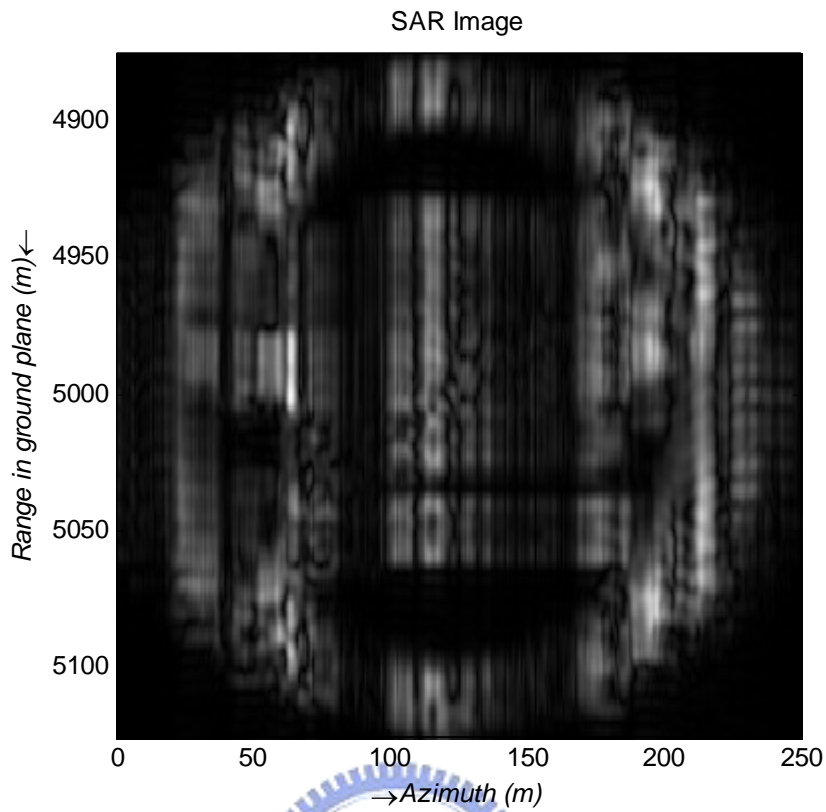
**Figure 4-17 Actual and nominal flight path.**



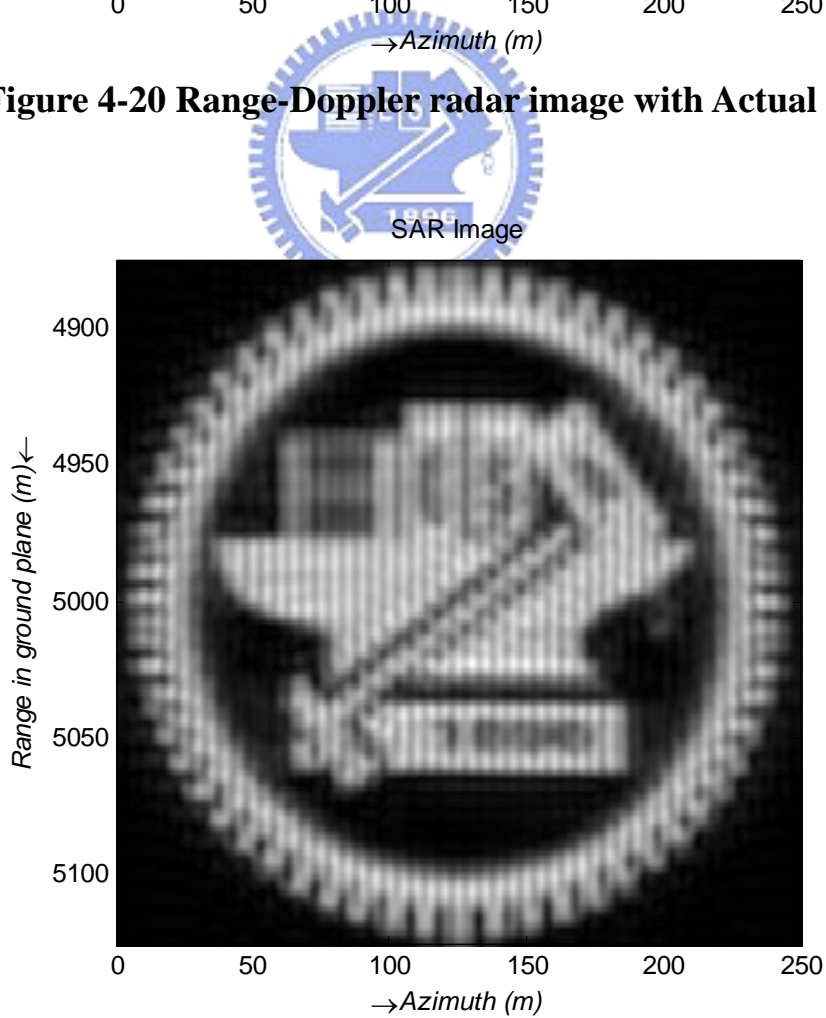
**Figure 4-18** The image after range compression with nominal path.



**Figure 4-19** Range-Doppler radar image with nominal path.



**Figure 4-20 Range-Doppler radar image with Actual path.**



**Figure 4-21 Range-Doppler radar image after LOS compensation.**

Pulsewidth	2us
Bandwidth	15MHz
Carrier frequency	2.4GHz
Receive window	Rmin = 5000 (m), Rmax =10000(m)
Number of target	4
Target range	[5500 7500 8500 9000] (m)
Target RCS	[1 0.3 0.5 0.7]

**Table 2-1 Parameters for range processing.**



Azimuth resolution	5m
Carrier frequency	2.4GHz
Aircraft velocity	10m/s
Slant range	5000m
Number of target	2
Target area	Xmin = -50m, Xmax = 50m
Target location	[-40 30] (m)
Target RCS	[1 0.5]

**Table 3-1 Parameters for azimuth processing.**

Target location	$(x, y) = (0, 5000)$ (m)
Target RCS	1
Range resolution	5m
Azimuth resolution	5m
Pulsewidth	2us
Bandwidth	30MHz
Carrier Frequency	2.4GHz
Receive window	$R_{min} = 4950\text{m}, R_{max} = 5050\text{m}$
Aircraft velocity	10m/s
Height	500m

**Table 4-1 Parameters for one point target simulation.**

Target location	$(x, y) = (-20, 4955), (0, 4955), (20, 4955), (-20, 4975), (20, 4975), (-20, 4995), (0, 4995), (20, 4995), (0, 5005), (-14.2, 5010.8), (14.2, 5010.8), (-20, 5025), (20, 5025), (-14.2, 5039.2), (14.2, 5039.2), (0, 5045)$ (m)
Target RCS	16
Range resolution	5m
Azimuth resolution	5m
Pulsewidth	2us
Bandwidth	30MHz
Carrier Frequency	2.4GHz
Receive window	$R_{min} = 4950\text{m}, R_{max} = 5050\text{m}$
Aircraft velocity	10m/s
Height	500m

**Table 4-2 Parameters for multiple point target simulation.**

Range resolution	5m
Azimuth resolution	5m
Pulsewidth	2us
Bandwidth	30MHz
Carrier Frequency	2.4GHz
Receive window	Rmin = 4875m, Rmax =5125m
Aircraft velocity	10m/s
Height	500m

**Table 4-3 Parameters for scenery simulation.**

